ORIGINAL ARTICLE

lajss.org
Latin American Journal of Solids and Structures

www.lajss.org

# Study on vibration isolation performance of composite multilayer wave impeding block based on wave impedance ratio under an underground dynamic load

**Meng Zhang[a], Qiang Ma[a,b*]**

[a]School of Civil Engineering, Qinghai University, Xining 810016, China. Email: 15133839505@163.com, maqiang0104@163.com
[b]Qinghai Provincial Key Laboratory of Energy-saving Building Materials and Engineering Safety, Xining 810016, China.

*Corresponding author

https://doi.org/10.1590/1679-78257439

## Abstract

Based on the theory of single-phase elastic medium and unsaturated porous medium, the vibration isolation effect of composite multilayer wave impeding block (WIB) in the unsaturated ground under an underground dynamic load is investigated. The results show that the best vibration isolation effect can be obtained by designing the wave impedance ratio between the composite multilayer WIB and unsaturated ground. The composite multilayer WIB improves the vibration-damping bandwidth compared with the homogeneous WIB. The vibration isolation effect is better the closer the embedded depth of the composite multilayer WIB is to the vibration source, and its vibration isolation effect increases significantly with the increase of thickness, but when the thickness of the WIB exceeds a certain critical thickness, its vibration isolation effect decreases with the increase of thickness. Soil saturation has a significant effect on the vibration isolation effect of composite multilayer WIB in the unsaturated ground, and the composite multilayer WIB can achieve a better vibration isolation effect at low saturation.

## Keywords

Underground dynamic load, unsaturated soil, composite multilayer WIB, wave impedance ratio, vibration isolation design

## Graphical Abstract

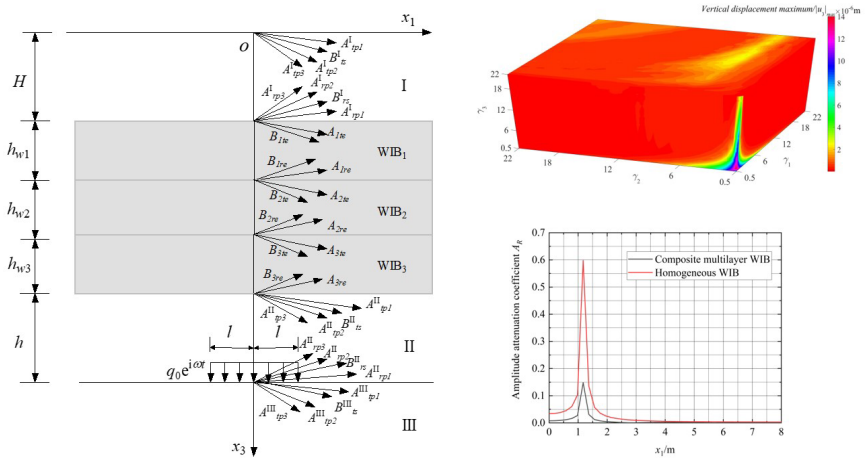


Received: January 10, 2023. In revised form: January 28, 2023. Accepted: February 08, 2023. Available online: February 10, 2023.
https://doi.org/10.1590/1679-78257439

## 1 INTRODUCTION

Internationally, vibration pollution has been listed as one of the seven environmental hazards and has begun to study the laws of vibration pollution, the causes of its generation, the ways of its propagation, and the methods of its control. As the environmental vibration generated during the work of underground rail transit and other engineering activities has many adverse effects on various precision instruments as well as people's living and working environments. Therefore, it is of great practical significance to find effective vibration damping and vibration isolation measures for ground vibration caused by underground dynamic loads, and ground vibration and its control have become one of the important topics that need to be urgently solved in the field of geotechnical engineering research.

The propagation process and attenuation law of ground vibration vary in different sites, and a series of important research results have been conducted by domestic and foreign scholars from various aspects such as load types and ground characteristics (Zienkiewicz et al., 1980; Zhou et al., 2015; Shi et al., 2021; Huang et al., 2022). The establishment of a barrier between the existing vibration source and the protected area to cut off the propagation path of elastic waves, attenuate the vibration energy and reduce the vibration amplitude is a commonly adopted vibration isolation measure internationally. At present, scholars at home and abroad have carried out a lot of research work on the vibration reduction performance of various vibration isolation barriers (Woods., 1968; Xu et al., 2015; Schevenels and Lombaert, 2017; Gao, 1998; Gao et al., 2018; Liu et al., 2019; Li et al., 2021; Ba et al., 2022). Among them, according to the form of vibration isolation barriers, Gao (1998) further classified barriers into continuous barriers and discontinuous barriers according to their geometric characteristics.

Chouw et al. (1991) were the first to analyze the active and passive vibration isolation effects of WIB in the elastic ground, and the results showed that the vibration isolation effect of WIB was better than that of filled trenches. Takemiya and Fujiwara (1994) studied the vibration isolation effect of group pile foundation excitation in a single soil layer on bedrock, and the results showed that the WIB is an effective vibration isolation measure. Gao and Li (2005); Gao et al. (2007) analyzed the vibration isolation effect of WIB in two-dimensional elastic foundations as well as two-dimensional laminated elastic foundations, and the study showed that the vibration isolation effect of WIB is significantly affected by the elastic modulus. Most of the materials of WIB in the above studies are relatively single, and the materials are mainly concentrated in single-phase solid media, and there is less research on the composite mode of WIB and non-uniform materials. Ma (2018), Ma et al. (2017) established a ground vibration isolation system with a functional gradient WIB in an elastic ground, and the study showed that the gradient WIB can effectively reduce the vibration amplitude. Gao et al. (2020, 2021) proposed a joint vibration isolation method combining Duxseal industrial filler and WIB (referred to as DXWIB), and found that the DXWIB barrier enhanced the bandwidth of traditional homogeneous WIB vibration reduction through experimental studies. Zhou et al. (2020) proposed a new type of combined air trench-WIB vibration isolation barrier and analyzed its vibration isolation performance in elastic foundations, which showed that the combined air trench-WIB vibration isolation barrier combined the respective advantages of air trench and WIB and could effectively control the foundation vibration caused by different frequency vibration sources. Due to the complexity of the soil, simplifying to a single elastic foundation does not fully reflect the true state of the soil. Gao et al. (2014) studied the vibration isolation performance of WIB in the saturated ground under the effect of rail traffic load for the saturated ground model. Gao et al. (2017) studied the vibration isolation effect of WIB in saturated soil and analyzed the saturated soil-foundation-WIB interaction. Based on the Biot theory of saturated porous media, Ma et al. (2019) investigated the vibration isolation effect of liquid-containing saturated porous gradient WIB in the saturated ground under a moving load. Subsequently, Shu et al. (2022) extended the soil type to unsaturated soils and investigated the propagation characteristics of $P_1$ waves through single-layer homogeneous WIB in unsaturated soils, and the results showed that the selection of shear modulus and density of WIB in the appropriate range can achieve better vibration isolation effects in the unsaturated ground.

As can be seen above, most of the current research on WIB vibration barriers is focused on single-phase elastic ground and saturated ground. However, natural soil in nature is generally a porous multiphase medium composed of solid-liquid-gas phases, and unsaturated soil is the more common state of existence in nature. Therefore, it is of more general significance to study the vibration damping and isolation effect of WIB in unsaturated soil ground. In addition, most of the previous studies on WIB vibration isolation barriers were limited to homogeneous WIB, and it was found that (Chouw et al., 1991; Takemiya and Fujiwara, 1994; Gao and Li, 2005; Gao et al., 2007) single-layer homogeneous WIB vibration isolation barriers have a good vibration isolation effect for a low-frequency vibration, but the deficiency of vibration amplification will occur for medium and high-frequency vibration.

Therefore, this paper proposes a new vibration isolation system with a composite multilayer WIB as a vibration isolation barrier based on the property that the greater the interfacial difference of thin layer media the more significant the vibration wave transmission and reflection effect, and studies the vibration isolation performance of the composite

multilayer WIB in the unsaturated ground. Based on the governing equations of unsaturated porous media, the mathematical model of composite multilayer WIB in the unsaturated ground under an underground dynamic load is established, and the general solution of displacement and stress of soil body in the domain of Fourier transform is derived by using Fourier transform and Helmholtz vector decomposition. The influence of the wave impedance between the material layers on the vibration isolation effect of the composite multilayer WIB is analyzed by numerical calculation, and the vibration isolation effect of the composite multilayer WIB and the homogeneous WIB in the unsaturated soil foundation is compared.

## 2 Mathematical model of the problem

The unsaturated ground is internally considered to be subjected to a vertical strip harmonic load is $q_0 e^{i\omega t}$ with an angular frequency is $\omega$ and amplitude is $q_0$ as shown in Figure 1. A composite multilayer WIB with thicknesses $h_{w1}$, $h_{w2}$, and $h_{w3}$ is set at a depth of $H$ from the surface of the unsaturated ground, and the composite multilayer WIB are located in the areas of $WIB_1$, $WIB_2$, $WIB_3$, respectively. The distance of the vibration source from the WIB is $h$. The composite multilayer WIB and the vibration source divide the unsaturated ground into three parts, **I**, **II**, and **III.** A schematic diagram of the wave propagation and the wave amplitude is given in the figure.

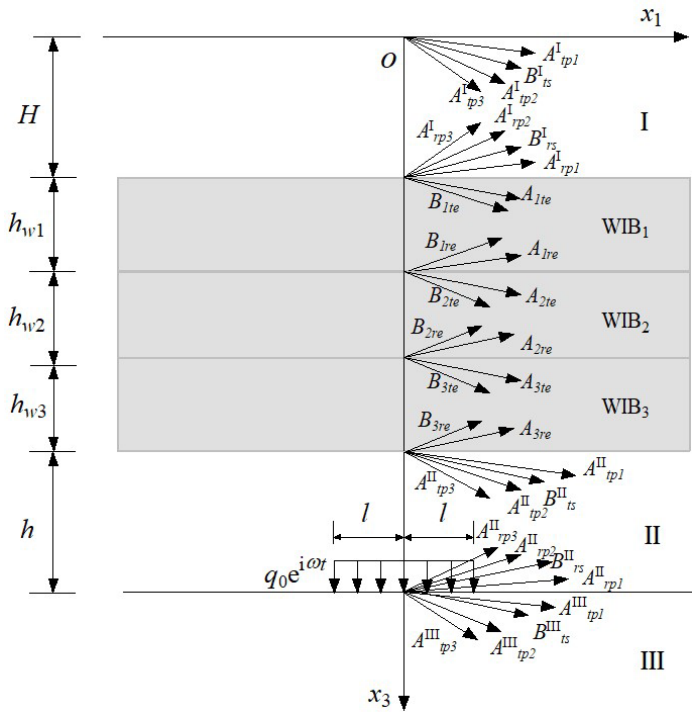


**Figure 1** Wave propagation diagram of WIB in unsaturated soil under an underground dynamic load.

## 3 Governing equations

### 3.1 *Single-phase solid medium*

Governing equations for an isotropic linear elastic single-phase continuous solid medium are as follows:

$$\left(\lambda_e + \mu_e\right)\nabla\left(\nabla \cdot \mathbf{u}^e\right) + \mu_e \nabla^2 \mathbf{u}^e = \rho_e \ddot{\mathbf{u}}^e \tag{1}$$

where $\lambda_e$ and $\mu_e$ denote the Lame elastic constants of the solid material, $\rho_e$ is the density of the solid material, $\mathbf{u}^e$ denotes the displacement vector.

The corresponding stress-displacement relation is as follows:

$$\boldsymbol{\sigma}^e = \lambda_e \left( \nabla \cdot \mathbf{u}^e \right) \mathbf{I} + \mu_e \left( \nabla \mathbf{u}^e + \mathbf{u}^e \nabla \right) \mathbf{I} \tag{2}$$

where $\boldsymbol{\sigma}^e$ denotes the stress tensor in a single-phase elastic solid, $\mathbf{I}$ is the unit matrix.

According to the Helmholtz vector decomposition, the displacement vector can be expressed as a potential function as follows:

$$\mathbf{u}^e = \nabla \varphi_e + \nabla \times \psi_e \tag{3}$$

where $\varphi_e$ and $\psi_e$ are the scalar potential function and vector potential function of the single-phase solid, respectively.

Substituting Eq. (3) into Eq. (1), the single-phase solid wave equation is as follows:

$$\nabla^2 \varphi_e = \frac{1}{v_p^2} \frac{\partial^2 \varphi_e}{\partial t^2}, \ \nabla^2 \psi_e = \frac{1}{v_s^2} \frac{\partial^2 \psi_e}{\partial t^2} \tag{4}$$

where $v_p = \sqrt{\left( \lambda_e + 2\mu_e \right) / \rho_e}$ and $v_s = \sqrt{\mu_e / \rho_e}$ are the propagation velocity of the longitudinal and transverse waves, respectively.

### 3.2 *Unsaturated porous medium*

Based on the fact that the model built in this paper is considered to be subjected to simple harmonic loading, all variables in the steady-state case can be written as follows:

$$f\left( x_1, x_3, t \right) = f\left( x_1, x_3 \right)^* \mathrm{e}^{\mathrm{i}\omega t} \tag{5}$$

where $f\left( x_1, x_3, t \right)$ is the functional form of all variables in a steady state, and $\omega$ is the circular frequency.

For convenience, the asterisk is omitted in the following derivation process.

Based on the theory of continuous medium mechanics and Bishop's effective stress formula, the dynamic governing equations of unsaturated soil were proposed by Xu and Wei (2011) as follows:

$$\mu_p \nabla^2 \mathbf{u}^s + \left( \lambda_p + \mu_p \right) \nabla \nabla \cdot \mathbf{u}^s - a\gamma \nabla p^l - a\left( 1 - \gamma \right) \nabla p^g = -\omega^2 \overline{\rho}_s \mathbf{u}^s - \omega^2 \overline{\rho}_l \mathbf{u}^l - \omega^2 \overline{\rho}_g \mathbf{u}^g \tag{6a}$$

$$-\nabla p^l = b^l \mathrm{i}\omega \left( \mathbf{u}^l - \mathbf{u}^s \right) - \omega^2 \rho_l \mathbf{u}^l \tag{6b}$$

$$-\nabla p^g = b^g \mathrm{i}\omega \left( \mathbf{u}^g - \mathbf{u}^s \right) - \omega^2 \rho_g \mathbf{u}^g \tag{6c}$$

$$-p^l = a_{11} \nabla \cdot \mathbf{u}^s + a_{12} \nabla \cdot \mathbf{u}^l + a_{13} \nabla \cdot \mathbf{u}^g \tag{6d}$$

$$-p^g = a_{21} \nabla \cdot \mathbf{u}^s + a_{22} \nabla \cdot \mathbf{u}^l + a_{23} \nabla \cdot \mathbf{u}^g \tag{6e}$$

where the coefficients (Xu and Wei, 2011) of $a_{11} \sim a_{23}$, $A_{11} \sim A_{23}$, $b^l$, $b^g$, $a$, $\gamma$, etc. are the corresponding coefficients in the governing equations for unsaturated porous media. $\mathbf{u}^s$, $\mathbf{u}^l$, $\mathbf{u}^g$, $\overline{\rho}_s = \left( 1 - n \right) \rho_s$, $\overline{\rho}_l = n S_r \rho_l$ and $\overline{\rho}_g = n\left( 1 - S_r \right) \rho_g$ are the displacements and relative densities of the solid, liquid, and gas phases of the unsaturated

soil, respectively. $\rho_s$, $\rho_l$ and $\rho_g$ are the densities of the solid, liquid, and gas phases, respectively. $\omega = 2\pi f$ is the angular frequency, $f$ is the frequency, *n* is the porosity, $S_r$ is the saturation, $\lambda_p$ and $\mu_p$ are the Lame coefficients of the unsaturated soil. $p^l$ and $p^g$ are the pore water and pore gas pressures, respectively.

The stress-strain relationship of unsaturated soil is as follows:

$$\sigma_{ij} = \lambda_p e\delta_{ij} + 2\mu_p\varepsilon_{ij} - \delta_{ij}ap \tag{7}$$

where $\sigma_{ij}$ is the total stress component of the unsaturated soil medium (*i*=*j*=1,3), $e = \nabla\cdot\mathbf{u}^s$ is the volumetric strain of the soil skeleton, $\delta_{ij}$ is the Kronecker symbol, $\varepsilon_{ij}$ is the strain of the soil skeleton, and $p = \gamma p^l + \left(1-\gamma\right)p^g$ is the equivalent pore fluid pressure.

Substituting Eqs. (6d) and (6e) into Eqs. (6a), (6b), and (6c) yields

$$\mu_p\nabla^2\mathbf{u}^s + B_1\nabla\left(\nabla\cdot\mathbf{u}^s\right) + B_2\nabla\left(\nabla\cdot\mathbf{u}^l\right) + B_3\nabla\left(\nabla\cdot\mathbf{u}^g\right) = -\omega^2\overline{\rho}_s\mathbf{u}^s - \omega^2\overline{\rho}_l\mathbf{u}^l - \omega^2\overline{\rho}_g\mathbf{u}^g \tag{8a}$$

$$a_{11}\nabla\left(\nabla\cdot\mathbf{u}^s\right) + a_{12}\nabla\left(\nabla\cdot\mathbf{u}^l\right) + a_{13}\nabla\left(\nabla\cdot\mathbf{u}^g\right) = C_1\mathbf{u}^s + C_2\mathbf{u}^l \tag{8b}$$

$$a_{21}\nabla\left(\nabla\cdot\mathbf{u}^s\right) + a_{22}\nabla\left(\nabla\cdot\mathbf{u}^l\right) + a_{23}\nabla\left(\nabla\cdot\mathbf{u}^g\right) = C_3\mathbf{u}^s + C_4\mathbf{u}^g \tag{8c}$$

where $B_1 = \lambda_p + \mu_p + a\gamma a_{11} + a\left(1-\gamma\right)a_{21}$, $B_2 = a\gamma a_{12} + a\left(1-\gamma\right)a_{22}$, $B_3 = a\gamma a_{13} + a\left(1-\gamma\right)a_{23}$, $C_1 = -b^l\mathrm{i}\omega$, $C_2 = b^1 i\omega - \omega^2\rho_1$, $C_3 = -b^g\mathrm{i}\omega$, $C_4 = b^g\mathrm{i}\omega - \omega^2\rho_g$.

According to the Helmholtz vector decomposition, the displacement vectors $\mathbf{u}^s$, $\mathbf{u}^l$, and $\mathbf{u}^g$ can be expressed in terms of potential functions as follows:

$$\mathbf{u}^z = \nabla\varphi_z + \nabla\times\psi_z \tag{9}$$

where (*z*=*s*, *l*, *g*). $\varphi_s$, $\varphi_l$, $\varphi_g$ are the scalar potential functions of solid, liquid, and gas phases, respectively. $\psi_s$, $\psi_l$, $\psi_g$ are the vector potential functions of solid, liquid, and gas phases, respectively.

Substituting Eq. (9) into Eqs. (8a~8c) for divergence and curl operations yields:

$$\left(\mu_p + B_1\right)\nabla^2\varphi_s + B_2\nabla^2\varphi_l + B_3\nabla^2\varphi_g = -\omega^2\overline{\rho}_s\varphi_s - \omega^2\overline{\rho}_l\varphi_l - \omega^2\overline{\rho}_g\varphi_g \tag{10a}$$

$$a_{11}\nabla^2\varphi_s + a_{12}\nabla^2\varphi_l + a_{13}\nabla^2\varphi_g = C_1\varphi_s + C_2\varphi_l \tag{10b}$$

$$a_{21}\nabla^2\varphi_s + a_{22}\nabla^2\varphi_l + a_{23}\nabla^2\varphi_g = C_3\varphi_s + C_4\varphi_g \tag{10c}$$

$$\mu_p\nabla^2\psi_s = -\omega^2\overline{\rho}_s\psi_s - \omega^2\overline{\rho}_l\psi_l - \omega^2\overline{\rho}_g\psi_g \tag{10d}$$

$$C_1\psi_s + C_2\psi_l = 0 \tag{10e}$$

$$C_3\psi_s + C_4\psi_g = 0 \tag{10f}$$

## 4 Solution of the displacement potential function

### 4.1 *Solution of single-phase solid medium*

The Fourier transform with respect to $x_1$ is defined as follows:

$$\tilde{f}\left(\xi, x_3\right)=\int_{-\infty}^{\infty} f\left(x_1, x_3\right) \mathrm{e}^{-\mathrm{i} \xi x_1} \mathrm{d} x_1 \tag{11}$$

where $\xi$ are the wave numbers in the $x_1$ direction.

Substituting Eqs. (5) and (11) into Eq. (4), after Fourier transforms yields:

$$\frac{\mathrm{d}^2 \tilde{\varphi}_e}{\mathrm{d} x_3^2}+\alpha_e^2 \tilde{\varphi}_e=0, \frac{\mathrm{d}^2 \tilde{\psi}_e}{\mathrm{d} x_3^2}+\beta_e^2 \tilde{\psi}_e=0 \tag{12}$$

where $\alpha_e=\sqrt{\omega^2 / v_p^2-\xi^2}$, $\beta_e=\sqrt{\omega^2 / v_s^2-\xi^2}$.

Therefore, the general solution of displacement potential function in a single-phase elastic solid medium can be obtained as follows:

$$\tilde{\varphi}_e=A_{te} \mathrm{e}^{-\mathrm{i} \alpha_e x_3}+A_{re} \mathrm{e}^{\mathrm{i} \alpha_e x_3}, \tilde{\psi}_e=B_{te} \mathrm{e}^{-\mathrm{i} \beta_e x_3}+B_{re} \mathrm{e}^{\mathrm{i} \beta_e x_3} \tag{13}$$

where $A_{te}$ and $A_{re}$ are the amplitudes of the transmitted P wave and reflected P wave in a single-phase solid medium respectively. $B_{te}$ and $B_{re}$ are the amplitudes of transmitted S wave and reflected S wave in a single-phase solid medium, respectively.

### 4.2 *Solution of the unsaturated porous medium*

Substituting Eq. (11) into Eqs. (10a~10c), after Fourier transforms yields:

$$\left(\mu_p+B_1\right) \frac{\mathrm{d}^2 \tilde{\varphi}_s}{\mathrm{d} x_3^2}+b_{11} \tilde{\varphi}_s+B_2 \frac{\mathrm{d}^2 \tilde{\varphi}_l}{\mathrm{d} x_3^2}+b_{12} \tilde{\varphi}_l+B_3 \frac{\mathrm{d}^2 \tilde{\varphi}_g}{\mathrm{d} x_3^2}+b_{13} \tilde{\varphi}_g=0 \tag{14a}$$

$$a_{11} \frac{\mathrm{d}^2 \tilde{\varphi}_s}{\mathrm{d} x_3^2}+b_{21} \tilde{\varphi}_s+a_{12} \frac{\mathrm{d}^2 \tilde{\varphi}_l}{\mathrm{d} x_3^2}+b_{22} \tilde{\varphi}_l+a_{13} \frac{\mathrm{d}^2 \tilde{\varphi}_g}{\mathrm{d} x_3^2}+b_{23} \tilde{\varphi}_g=0 \tag{14b}$$

$$a_{21} \frac{\mathrm{d}^2 \tilde{\varphi}_s}{\mathrm{d} x_3^2}+b_{31} \tilde{\varphi}_s+a_{22} \frac{\mathrm{d}^2 \tilde{\varphi}_l}{\mathrm{d} x_3^2}+b_{32} \tilde{\varphi}_l+a_{23} \frac{\mathrm{d}^2 \tilde{\varphi}_g}{\mathrm{d} x_3^2}+b_{33} \tilde{\varphi}_g=0 \tag{14c}$$

where $b_{11}=\overline{\rho}_s \omega^2-\left(\mu_p+B_1\right) \xi^2$, $b_{12}=\overline{\rho}_l \omega^2-B_2 \xi^2$, $b_{13}=\overline{\rho}_g \omega^2-B_3 \xi^2$, $b_{21}=-C_1-a_{11} \xi^2$, $b_{22}=-C_2-a_{12} \xi^2$, $b_{23}=-a_{13} \xi^2$, $b_{31}=-C_3-a_{21} \xi^2$, $b_{32}=-a_{22} \xi^2$, $b_{33}=-C_4-a_{23} \xi^2$.

Assuming that the solution of the Eqs. (14) as follows:

$$\left[\tilde{\varphi}_s \quad \tilde{\varphi}_l \quad \tilde{\varphi}_g\right]^{\mathrm{T}}=\left[c^s \quad c^l \quad c^g\right]^{\mathrm{T}} \exp\left(\lambda x_3\right) \tag{15}$$

Substituting Eq. (15) into Eqs. (14) yields the linear equations as follows:

$$\begin{bmatrix} \lambda^2 B_3 + b_{13} & \lambda^2 B_2 + b_{12} & \lambda^2(\mu_p + B_1) + b_{11} \\ \lambda^2 a_{13} + b_{23} & \lambda^2 a_{12} + b_{22} & \lambda^2 a_{11} + b_{21} \\ \lambda^2 a_{23} + b_{33} & \lambda^2 a_{22} + b_{32} & \lambda^2 a_{21} + b_{31} \end{bmatrix} \begin{bmatrix} c^g \\ c^l \\ c^s \end{bmatrix} = 0 \tag{16}$$

The condition that Eq. (16) has a non-zero solution is that the determinant of its coefficient matrix is 0, namely:

$$\beta_1 \lambda^6 + \beta_2 \lambda^4 + \beta_3 \lambda^2 + \beta_4 = 0 \tag{17}$$

where $\beta_n \left(n = 1,2,3,4\right)$ are detailed in Appendix A.

The roots of Eq. (17) are $\pm\lambda_n \left(n = 1,2,3\right)$, $\lambda_n$ are given by the following equation:

$$\lambda_n = \sqrt{r_n} \left(\mathrm{Re}\left[\lambda_n\right] \geq 0, n = 1,2,3\right) \tag{18}$$

where $r_n$ are determined by the equation $\beta_1 r_n^3 + \beta_2 r_n^2 + \beta_3 r_n + \beta_4 = 0$.

The solution of ordinary differential Eqs. (14) can be obtained as follows:

$$\tilde{\varphi}_s = \sum_{n=1}^{3} A_{tpn} \mathrm{e}^{-\lambda_n x_3} + A_{rpn} \mathrm{e}^{\lambda_n x_3} \tag{19a}$$

$$\tilde{\varphi}_l = \sum_{n=1}^{3} \delta_{pn}^l \left( A_{tpn} \mathrm{e}^{-\lambda_n x_3} + A_{rpn} \mathrm{e}^{\lambda_n x_3} \right) \tag{19b}$$

$$\tilde{\varphi}_g = \sum_{n=1}^{3} \delta_{pn}^g \left( A_{tpn} \mathrm{e}^{-\lambda_n x_3} + A_{rpn} \mathrm{e}^{\lambda_n x_3} \right) \tag{19c}$$

where $\delta_{pn}^l = -\dfrac{\left(B_1 a_{13} - B_3 a_{11} + a_{13}\mu_p\right) r_n^2 + \left(B_1 b_{23} - B_3 b_{21} - a_{11} b_{13} + a_{13} b_{11} + b_{23}\mu_p\right) r_n + b_{11} b_{23} - b_{13} b_{21}}{\left(B_2 a_{13} - B_3 a_{12}\right) r_n^2 + \left(B_2 b_{23} - B_3 b_{22} - a_{12} b_{13} + a_{13} b_{12}\right) r_n + b_{12} b_{23} - b_{13} b_{22}}$,

$\delta_{pn}^g = \dfrac{\left(B_1 a_{12} - B_2 a_{11} + a_{12}\mu_p\right) r_n^2 + \left(B_1 b_{22} - B_2 b_{21} - a_{11} b_{12} + a_{12} b_{11} + b_{22}\mu_p\right) r_n + b_{11} b_{22} - b_{12} b_{21}}{\left(B_2 a_{13} - B_3 a_{12}\right) r_n^2 + \left(B_2 b_{23} - B_3 b_{22} - a_{12} b_{13} + a_{13} b_{12}\right) r_n + b_{12} b_{23} - b_{13} b_{22}}$, $A_{tpn}$ and $A_{rpn}$ (n=1,2,3) are the amplitudes of transmitted $P_1$ wave, $P_2$ wave, $P_3$ wave and reflected $P_1$ wave, $P_2$ wave, and $P_3$ wave in unsaturated soil porous medium, respectively.

Substituting Eq. (11) into Eqs. (10d~10f), then performing the Fourier transform on them yields:

$$\mu_p \frac{\mathrm{d}^2 \tilde{\psi}_s}{\mathrm{d}x_3^2} + d_{11} \tilde{\psi}_s + d_{12} \tilde{\psi}_l + d_{13} \tilde{\psi}_g = 0 \tag{20a}$$

$$d_{21} \tilde{\psi}_s + d_{22} \tilde{\psi}_l = 0 \tag{20b}$$

$$d_{31} \tilde{\psi}_s + d_{32} \tilde{\psi}_l = 0 \tag{20c}$$

where $d_{11} = \overline{\rho}_s\omega^2 - \mu_p\xi^2$, $d_{12} = \overline{\rho}_l\omega^2$, $d_{13} = \overline{\rho}_g\omega^2$, $d_{21} = C_1$, $d_{22} = C_2$, $d_{31} = C_3$, $d_{32} = C_4$.

Assuming that the solution of the Eqs. (20) as follows:

$$\begin{bmatrix}\tilde{\psi}_s & \tilde{\psi}_l & \tilde{\psi}_g\end{bmatrix}^{\mathrm{T}} = \begin{bmatrix}d^s & d^l & d^g\end{bmatrix}^{\mathrm{T}}\exp\left(rx_3\right) \tag{21}$$

Substituting Eq. (21) into Eqs. (20) yields the linear equations:

$$\begin{bmatrix} d_{13} & d_{12} & \mu_p r^2 + d_{11} \\ 0 & d_{22} & d_{21} \\ d_{33} & 0 & d_{31} \end{bmatrix}\begin{bmatrix} d^g \\ d^l \\ d^s \end{bmatrix} = 0 \tag{22}$$

The condition that Eq. (22) has a non-zero solution is that the determinant of its coefficient matrix is 0, namely:

$$\beta_5 r^2 + \beta_6 = 0 \tag{23}$$

The roots of Eq. (23) are $\pm r$, $r$ is then given by the following equation:

$$r = \sqrt{-\beta_6 \,/\, \beta_5}\left(\mathrm{Re}\left[r\right] \geq 0\right) \tag{24}$$

where $\beta_n\left(n = 5,6\right)$ are detailed in Appendix A.

The solution of ordinary differential Eqs. (20) can be obtained as follows:

$$\tilde{\psi}_s = B_{ts}\mathrm{e}^{-rx_3} + B_{rs}\mathrm{e}^{rx_3} \tag{25a}$$

$$\tilde{\psi}_l = \delta_s^l\left(B_{ts}\mathrm{e}^{-rx_3} + B_{rs}\mathrm{e}^{rx_3}\right) \tag{25b}$$

$$\tilde{\psi}_g = \delta_s^g\left(B_{ts}\mathrm{e}^{-rx_3} + B_{rs}\mathrm{e}^{rx_3}\right) \tag{25c}$$

where $\delta_s^l = -\dfrac{d_{21}}{d_{22}}$, $\delta_s^g = \dfrac{d_{12}d_{21} - (\mu_p r^2 + d_{11})d_{22}}{d_{13}d_{22}}$. $B_{ts}$ and $B_{rs}$ are the amplitudes of transmission and reflection waves of unsaturated porous media, respectively.

## 5 Solving the dynamic response problem of unsaturated ground

### 5.1 *Dynamic response of unsaturated ground*

In the coordinate system $\left(x_1, x_3\right)$, each displacement component can be expressed by the displacement potential functions $\varphi$ and $\psi$ as follows:

$$u_1 = \frac{\partial\varphi}{\partial x_1} - \frac{\partial\psi}{\partial x_3},\ u_3 = \frac{\partial\varphi}{\partial x_3} + \frac{\partial\psi}{\partial x_1} \tag{26}$$

Substituting Eqs. (13) and (26) into Eqs. (2) and (3) and substituting Eqs. (19), (25), (26) into Eqs. (6d), (6e), (7), and (9), the displacement and stress expressions in the Fourier transform domain can be obtained for the elastic medium and the unsaturated porous medium, respectively.

In the region $0 \le x_3 \le H$:

$$\tilde{u}_1^{\mathrm{sI}} = \mathrm{i}\xi\left(\sum_{n=1}^{3} A_{tpn}^{\mathrm{I}} \mathrm{e}^{-\lambda_n x_3} + A_{rpn}^{\mathrm{I}} \mathrm{e}^{\lambda_n x_3}\right) + r\left(B_{ts}^{\mathrm{I}} \mathrm{e}^{-r x_3} - B_{rs}^{\mathrm{I}} \mathrm{e}^{r x_3}\right) \tag{27a}$$

$$\tilde{u}_3^{\mathrm{sI}} = \left[\sum_{n=1}^{3} -\lambda_n \left(A_{tpn}^{\mathrm{I}} \mathrm{e}^{-\lambda_n x_3} - A_{rpn}^{\mathrm{I}} \mathrm{e}^{\lambda_n x_3}\right)\right] + \mathrm{i}\xi\left(B_{ts}^{\mathrm{I}} \mathrm{e}^{-r x_3} + B_{rs}^{\mathrm{I}} \mathrm{e}^{r x_3}\right) \tag{27b}$$

$$\tilde{u}_1^{\mathrm{fI}} = \mathrm{i}\xi\left[\sum_{n=1}^{3} \delta_{pn}^{l} \left(A_{tpn}^{\mathrm{I}} \mathrm{e}^{-\lambda_n x_3} + A_{rpn}^{\mathrm{I}} \mathrm{e}^{\lambda_n x_3}\right)\right] + r\delta_s^{l}\left(B_{ts}^{\mathrm{I}} \mathrm{e}^{-r x_3} - B_{rs}^{\mathrm{I}} \mathrm{e}^{r x_3}\right) \tag{27c}$$

$$\tilde{u}_3^{\mathrm{fI}} = \left[\sum_{n=1}^{3} -\lambda_n \delta_{pn}^{l} \left(A_{tpn}^{\mathrm{I}} \mathrm{e}^{-\lambda_n x_3} - A_{rpn}^{\mathrm{I}} \mathrm{e}^{\lambda_n x_3}\right)\right] + \mathrm{i}\xi\delta_s^{l}\left(B_{ts}^{\mathrm{I}} \mathrm{e}^{-r x_3} + B_{rs}^{\mathrm{I}} \mathrm{e}^{r x_3}\right) \tag{27d}$$

$$\tilde{u}_1^{\mathrm{gI}} = \mathrm{i}\xi\left[\sum_{n=1}^{3} \delta_{pn}^{g} \left(A_{tpn}^{\mathrm{I}} \mathrm{e}^{-\lambda_n x_3} + A_{rpn}^{\mathrm{I}} \mathrm{e}^{\lambda_n x_3}\right)\right] + r\delta_s^{g}\left(B_{ts}^{\mathrm{I}} \mathrm{e}^{-r x_3} - B_{rs}^{\mathrm{I}} \mathrm{e}^{r x_3}\right) \tag{27e}$$

$$\tilde{u}_3^{\mathrm{gI}} = \left[\sum_{n=1}^{3} -\lambda_n \delta_{pn}^{g} \left(A_{tpn}^{\mathrm{I}} \mathrm{e}^{-\lambda_n x_3} - A_{rpn}^{\mathrm{I}} \mathrm{e}^{\lambda_n x_3}\right)\right] + \mathrm{i}\xi\delta_s^{g}\left(B_{ts}^{\mathrm{I}} \mathrm{e}^{-r x_3} + B_{rs}^{\mathrm{I}} \mathrm{e}^{r x_3}\right) \tag{27f}$$

$$\tilde{\sigma}_{13}^{\mathrm{I}} = 2\mu_p \mathrm{i}\xi\left[\sum_{n=1}^{3} -\lambda_n \left(A_{tpn}^{\mathrm{I}} \mathrm{e}^{-\lambda_n x_3} - A_{rpn}^{\mathrm{I}} \mathrm{e}^{\lambda_n x_3}\right)\right] - \mu_p\left(r^2 + \xi^2\right)\left(B_{ts}^{\mathrm{I}} \mathrm{e}^{-r x_3} + B_{rs}^{\mathrm{I}} \mathrm{e}^{r x_3}\right) \tag{27g}$$

$$\tilde{\sigma}_{33}^{\mathrm{I}} = \left[\sum_{n=1}^{3} \chi_n \left(A_{tpn}^{\mathrm{I}} \mathrm{e}^{-\lambda_n x_3} + A_{rpn}^{\mathrm{I}} \mathrm{e}^{\lambda_n x_3}\right)\right] - 2\mathrm{i}\xi r\mu_p\left(B_{ts}^{\mathrm{I}} \mathrm{e}^{-r x_3} - B_{rs}^{\mathrm{I}} \mathrm{e}^{r x_3}\right) \tag{27h}$$

$$\tilde{p}^{\mathrm{fI}} = \sum_{n=1}^{3}\left(a_{11} + a_{12}\delta_{pn}^{l} + a_{13}\delta_{pn}^{g}\right)\left(\xi^2 - \lambda_n^2\right)\left(A_{tpn}^{\mathrm{I}} \mathrm{e}^{-\lambda_n x_3} + A_{rpn}^{\mathrm{I}} \mathrm{e}^{\lambda_n x_3}\right) \tag{27i}$$

$$\tilde{p}^{\mathrm{gI}} = \sum_{n=1}^{3}\left(a_{21} + a_{22}\delta_{pn}^{l} + a_{23}\delta_{pn}^{g}\right)\left(\xi^2 - \lambda_n^2\right)\left(A_{tpn}^{\mathrm{I}} \mathrm{e}^{-\lambda_n x_3} + A_{rpn}^{\mathrm{I}} \mathrm{e}^{\lambda_n x_3}\right) \tag{27j}$$

where $\chi_n = \left[a\gamma\left(a_{11} + a_{12}\delta_{pn}^{l} + a_{13}\delta_{pn}^{g}\right) + a\left(1-\gamma\right)\left(a_{21} + a_{22}\delta_{pn}^{l} + a_{23}\delta_{pn}^{g}\right)\right]\left(\lambda_n^2 - \xi^2\right) + \left[\left(\lambda_p + 2\mu_p\right)\lambda_n^2 - \lambda_p\xi^2\right]$.

In the region $H \le x_3 \le H + h_{w1}$:

$$\tilde{u}_1^{1e} = \mathrm{i}\xi\left(A_{1te} \mathrm{e}^{-\mathrm{i}\alpha_{1e} x_3} + A_{1re} \mathrm{e}^{\mathrm{i}\alpha_{1e} x_3}\right) + \mathrm{i}\beta_{1e}\left(B_{1te} \mathrm{e}^{-\mathrm{i}\beta_{1e} x_3} - B_{1re} \mathrm{e}^{\mathrm{i}\beta_{1e} x_3}\right) \tag{28a}$$

$$\tilde{u}_3^{1e} = -\mathrm{i}\alpha_{1e}\left(A_{1te} \mathrm{e}^{-\mathrm{i}\alpha_{1e} x_3} - A_{1re} \mathrm{e}^{\mathrm{i}\alpha_{1e} x_3}\right) + \mathrm{i}\xi\left(B_{1te} \mathrm{e}^{-\mathrm{i}\beta_{1e} x_3} + B_{1re} \mathrm{e}^{\mathrm{i}\beta_{1e} x_3}\right) \tag{28b}$$

$$\tilde{\sigma}_{13}^{1e} = 2\mu_{1e}\xi\alpha_{1e}\left(A_{1te}\mathrm{e}^{-\mathrm{i}\alpha_{1e}x_3} - A_{1re}\mathrm{e}^{\mathrm{i}\alpha_{1e}x_3}\right)+\mu_{1e}\left(\beta_{1e}{}^2\text{-}\xi^2\right)\left(B_{1te}\mathrm{e}^{-\mathrm{i}\beta_{1e}x_3} + B_{1re}\mathrm{e}^{\mathrm{i}\beta_{1e}x_3}\right) \tag{28c}$$

$$\tilde{\sigma}_{33}^{1e} = \left[-\lambda_{1e}\xi^2 - \alpha_{1e}{}^2\left(\lambda_{1e} + 2\mu_{1e}\right)\right]\left(A_{1te}\mathrm{e}^{-\mathrm{i}\alpha_{1e}x_3} + A_{1re}\mathrm{e}^{\mathrm{i}\alpha_{1e}x_3}\right) + 2\mu_{1e}\beta_{1e}\xi\left(B_{1te}\mathrm{e}^{-\mathrm{i}\beta_{1e}x_3} - B_{1re}\mathrm{e}^{\mathrm{i}\beta_{1e}x_3}\right) \tag{28d}$$

In the region $H+h_{w1} \le x_3 \le H+h_{w1}+h_{w2}$:

$$\tilde{u}_1^{2e} = \mathrm{i}\xi\left(A_{2te}\mathrm{e}^{-\mathrm{i}\alpha_{2e}x_3} + A_{2re}\mathrm{e}^{\mathrm{i}\alpha_{2e}x_3}\right)+\mathrm{i}\beta_{2e}\left(B_{2te}\mathrm{e}^{-\mathrm{i}\beta_{2e}x_3} - B_{2re}\mathrm{e}^{\mathrm{i}\beta_{2e}x_3}\right) \tag{29a}$$

$$\tilde{u}_3^{2e} = -\mathrm{i}\alpha_{2e}\left(A_{2te}\mathrm{e}^{-\mathrm{i}\alpha_{2e}x_3} - A_{2re}\mathrm{e}^{\mathrm{i}\alpha_{2e}x_3}\right) + \mathrm{i}\xi\left(B_{2te}\mathrm{e}^{-\mathrm{i}\beta_{2e}x_3} + B_{2re}\mathrm{e}^{\mathrm{i}\beta_{2e}x_3}\right) \tag{29b}$$

$$\tilde{\sigma}_{13}^{2e} = 2\mu_{2e}\xi\alpha_{2e}\left(A_{2te}\mathrm{e}^{-\mathrm{i}\alpha_{2e}x_3} - A_{2re}\mathrm{e}^{\mathrm{i}\alpha_{2e}x_3}\right)+\mu_{2e}\left(\beta_{2e}{}^2\text{-}\xi^2\right)\left(B_{2te}\mathrm{e}^{-\mathrm{i}\beta_{2e}x_3} + B_{2re}\mathrm{e}^{\mathrm{i}\beta_{2e}x_3}\right) \tag{29c}$$

$$\tilde{\sigma}_{33}^{2e} = \left[-\lambda_{2e}\xi^2 - \alpha_{2e}^2\left(\lambda_{2e} + 2\mu_{2e}\right)\right]\left(A_{2te}\mathrm{e}^{-\mathrm{i}\alpha_{2e}x_3} + A_{2re}\mathrm{e}^{\mathrm{i}\alpha_{2e}x_3}\right) + 2\mu_{2e}\beta_{2e}\xi\left(B_{2te}\mathrm{e}^{-\mathrm{i}\beta_{2e}x_3} - B_{2re}\mathrm{e}^{\mathrm{i}\beta_{2e}x_3}\right) \tag{29d}$$

In the region $H+h_{w1}+h_{w2} \le x_3 \le H+h_{w1}+h_{w2}+h_{w3}$:

$$\tilde{u}_1^{3e} = \mathrm{i}\xi\left(A_{3te}\mathrm{e}^{-\mathrm{i}\alpha_{3e}x_3} + A_{3re}\mathrm{e}^{\mathrm{i}\alpha_{3e}x_3}\right)+\mathrm{i}\beta_{3e}\left(B_{3te}\mathrm{e}^{-\mathrm{i}\beta_{3e}x_3} - B_{3re}\mathrm{e}^{\mathrm{i}\beta_{3e}x_3}\right) \tag{30a}$$

$$\tilde{u}_3^{3e} = -\mathrm{i}\alpha_{3e}\left(A_{3te}\mathrm{e}^{-\mathrm{i}\alpha_{3e}x_3} - A_{3re}\mathrm{e}^{\mathrm{i}\alpha_{3e}x_3}\right) + \mathrm{i}\xi\left(B_{3te}\mathrm{e}^{-\mathrm{i}\beta_{3e}x_3} + B_{3re}\mathrm{e}^{\mathrm{i}\beta_{3e}x_3}\right) \tag{30b}$$

$$\tilde{\sigma}_{13}^{3e} = 2\mu_{3e}\xi\alpha_{3e}\left(A_{3te}\mathrm{e}^{-\mathrm{i}\alpha_{3e}x_3} - A_{3re}\mathrm{e}^{\mathrm{i}\alpha_{3e}x_3}\right)+\mu_{3e}\left(\beta_{3e}^2\text{-}\xi^2\right)\left(B_{3te}\mathrm{e}^{-\mathrm{i}\beta_{3e}x_3} + B_{3re}\mathrm{e}^{\mathrm{i}\beta_{3e}x_3}\right) \tag{30c}$$

$$\tilde{\sigma}_{33}^{3e} = \left[-\lambda_{3e}\xi^2 - \alpha_{3e}{}^2(\lambda_{3e} + 2\mu_{3e})\right]\left(A_{3te}\mathrm{e}^{-\mathrm{i}\alpha_{3e}x_3} + A_{3re}\mathrm{e}^{\mathrm{i}\alpha_{3e}x_3}\right) + 2\mu_{3e}\beta_{3e}\xi\left(B_{3te}\mathrm{e}^{-\mathrm{i}\beta_{3e}x_3} - B_{3re}\mathrm{e}^{\mathrm{i}\beta_{3e}x_3}\right) \tag{30d}$$

In the region $H+h_{w1}+h_{w2}+h_{w3} \le x_3 \le H+h_{w1}+h_{w2}+h_{w3}+h$:

$$\tilde{u}_1^{\mathrm{sII}} = \mathrm{i}\xi\left(\sum_{n=1}^{3} A_{tpn}^{\mathrm{II}}\mathrm{e}^{-\lambda_n x_3} + A_{rpn}^{\mathrm{II}}\mathrm{e}^{\lambda_n x_3}\right) + r\left(B_{ts}^{\mathrm{II}}\mathrm{e}^{-rx_3} - B_{rs}^{\mathrm{II}}\mathrm{e}^{rx_3}\right) \tag{31a}$$

$$\tilde{u}_3^{\mathrm{sII}} = \left[\sum_{n=1}^{3} -\lambda_n\left(A_{tpn}^{\mathrm{II}}\mathrm{e}^{-\lambda_n x_3} - A_{rpn}^{\mathrm{II}}\mathrm{e}^{\lambda_n x_3}\right)\right] + \mathrm{i}\xi\left(B_{ts}^{\mathrm{II}}\mathrm{e}^{-rx_3} + B_{rs}^{\mathrm{II}}\mathrm{e}^{rx_3}\right) \tag{31b}$$

$$\tilde{u}_1^{\mathrm{II}} = \mathrm{i}\xi\left[\sum_{n=1}^{3} \delta_{pn}^{l}\left(A_{tpn}^{\mathrm{II}}\mathrm{e}^{-\lambda_n x_3} + A_{rpn}^{\mathrm{II}}\mathrm{e}^{\lambda_n x_3}\right)\right] + r\delta_s^l\left(B_{ts}^{\mathrm{II}}\mathrm{e}^{-rx_3} - B_{rs}^{\mathrm{II}}\mathrm{e}^{rx_3}\right) \tag{31c}$$

$$\tilde{u}_3^{\mathrm{II}} = \left[\sum_{n=1}^{3} -\lambda_n\delta_{pn}^{l}\left(A_{tpn}^{\mathrm{II}}\mathrm{e}^{-\lambda_n x_3} - A_{rpn}^{\mathrm{II}}\mathrm{e}^{\lambda_n x_3}\right)\right] + \mathrm{i}\xi\delta_s^l\left(B_{ts}^{\mathrm{II}}\mathrm{e}^{-rx_3} + B_{rs}^{\mathrm{II}}\mathrm{e}^{rx_3}\right) \tag{31d}$$

$$\tilde{u}_1^{g\mathrm{II}} = \mathrm{i}\xi\left[\sum_{n=1}^{3}\delta_{pn}^{g}\left(A_{tpn}^{\mathrm{II}}\mathrm{e}^{-\lambda_n x_3} + A_{rpn}^{\mathrm{II}}\mathrm{e}^{\lambda_n x_3}\right)\right] + r\delta_s^{g}\left(B_{ts}^{\mathrm{II}}\mathrm{e}^{-rx_3} - B_{rs}^{\mathrm{II}}\mathrm{e}^{rx_3}\right) \tag{31e}$$

$$\tilde{u}_3^{g\mathrm{II}} = \left[\sum_{n=1}^{3}-\lambda_n\delta_{pn}^{g}\left(A_{tpn}^{\mathrm{II}}\mathrm{e}^{-\lambda_n x_3} - A_{rpn}^{\mathrm{II}}\mathrm{e}^{\lambda_n x_3}\right)\right] + \mathrm{i}\xi\delta_s^{g}\left(B_{ts}^{\mathrm{II}}\mathrm{e}^{-rx_3} + B_{rs}^{\mathrm{II}}\delta_s^{g}\mathrm{e}^{rx_3}\right) \tag{31f}$$

$$\tilde{\sigma}_{13}^{\mathrm{II}} = 2\mu_p\mathrm{i}\xi\left[\sum_{n=1}^{3}-\lambda_n\left(A_{tpn}^{\mathrm{II}}\mathrm{e}^{-\lambda_n x_3} - A_{rpn}^{\mathrm{II}}\mathrm{e}^{\lambda_n x_3}\right)\right] - \mu_p\left(r^2+\xi^2\right)\left(B_{ts}^{\mathrm{II}}\mathrm{e}^{-rx_3} + B_{rs}^{\mathrm{II}}\mathrm{e}^{rx_3}\right) \tag{31g}$$

$$\tilde{\sigma}_{33}^{\mathrm{II}} = \left[\sum_{n=1}^{3}\chi_n\left(A_{tpn}^{\mathrm{II}}\mathrm{e}^{-\lambda_n x_3} + A_{rpn}^{\mathrm{II}}\mathrm{e}^{\lambda_n x_3}\right)\right] - 2\mathrm{i}\xi r\mu_p\left(B_{ts}^{\mathrm{II}}\mathrm{e}^{-rx_3} - B_{rs}^{\mathrm{II}}\mathrm{e}^{rx_3}\right) \tag{31h}$$

In the region $x_3 \geq H+h_{w1}+h_{w2}+h_{w3}+h$:

$$\tilde{u}_1^{s\mathrm{III}} = \mathrm{i}\xi\left(\sum_{n=1}^{3}A_{tpn}^{\mathrm{III}}\mathrm{e}^{-\lambda_n x_3}\right) + rB_{ts}^{\mathrm{III}}\mathrm{e}^{-rx_3} \tag{32a}$$

$$\tilde{u}_3^{s\mathrm{III}} = \left(\sum_{n=1}^{3}-\lambda_n A_{tpn}^{\mathrm{III}}\mathrm{e}^{-\lambda_n x_3}\right) + \mathrm{i}\xi B_{ts}^{\mathrm{III}}\mathrm{e}^{-rx_3} \tag{32b}$$

$$\tilde{\sigma}_{13}^{\mathrm{III}} = 2\mu_p\mathrm{i}\xi\left(\sum_{n=1}^{3}-\lambda_n A_{tpn}^{\mathrm{III}}\mathrm{e}^{-\lambda_n x_3}\right) - \mu_p\left(r^2+\xi^2\right)B_{ts}^{\mathrm{III}}\mathrm{e}^{-rx_3} \tag{32c}$$

$$\tilde{\sigma}_{33}^{\mathrm{III}} = \left(\sum_{n=1}^{3}\chi_n A_{tpn}^{\mathrm{III}}\mathrm{e}^{-\lambda_n x_3}\right) - 2\mathrm{i}\xi r\mu_p B_{ts}^{\mathrm{III}}\mathrm{e}^{-rx_3} \tag{32d}$$

### 5.2 *Boundary conditions and solution*

For the case where the load acts in the interior of the half-plane, the boundary conditions and the continuity conditions at the interfaces of the layers are as follows:

At $x_3 = 0$:

$$\tilde{\sigma}_{33}^{\mathrm{I}} = 0,\ \tilde{\sigma}_{13}^{\mathrm{I}} = 0,\ \tilde{p}^{\mathrm{II}} = 0,\ \tilde{p}^{g\mathrm{I}} = 0 \tag{33}$$

At $x_3 = H$:

$$\tilde{\sigma}_{33}^{\mathrm{I}} = \tilde{\sigma}_{33}^{1e},\tilde{\sigma}_{13}^{\mathrm{I}} = \tilde{\sigma}_{13}^{1e},\ \tilde{u}_3^{s\mathrm{I}} = \tilde{u}_3^{1e},\ \tilde{u}_1^{s\mathrm{I}} = \tilde{u}_1^{1e},\ \tilde{u}_3^{\mathrm{II}} = \tilde{u}_3^{s\mathrm{I}},\ \tilde{u}_3^{g\mathrm{I}} = \tilde{u}_3^{s\mathrm{I}},\ \tilde{u}_1^{\mathrm{II}} = \tilde{u}_1^{s\mathrm{I}},\ \tilde{u}_1^{g\mathrm{I}} = \tilde{u}_1^{s\mathrm{I}} \tag{34}$$

At $x_3 = H + h_{w1}$:

$$\tilde{\sigma}_{33}^{1e} = \tilde{\sigma}_{33}^{2e},\ \tilde{\sigma}_{13}^{1e} = \tilde{\sigma}_{13}^{2e},\ u_3^{1e} = u_3^{2e},\ u_1^{1e} = u_1^{2e} \tag{35}$$

At $x_3 = H + h_{w1} + h_{w2}$:

$$\tilde{\sigma}_{33}^{2e} = \tilde{\sigma}_{33}^{3e},\ \tilde{\sigma}_{13}^{2e} = \tilde{\sigma}_{13}^{3e},\ u_3^{2e} = u_3^{3e},\ u_1^{2e} = u_1^{3e} \tag{36}$$

At $x_3 = H+h_{w1} + h_{w2}+h_{w3}$:

$$\tilde{\sigma}_{33}^{3e} = \tilde{\sigma}_{33}^{\mathrm{II}},\ \tilde{\sigma}_{13}^{3e} = \tilde{\sigma}_{13}^{\mathrm{II}},\ \tilde{u}_3^{3e} = \tilde{u}_3^{\mathrm{sII}},\ \tilde{u}_1^{3e} = \tilde{u}_1^{\mathrm{sII}},\ \tilde{u}_3^{\mathrm{sII}} = \tilde{u}_3^{\mathrm{fII}},\ \tilde{u}_3^{\mathrm{sII}} = \tilde{u}_3^{\mathrm{gII}},\ \tilde{u}_1^{\mathrm{sII}} = \tilde{u}_1^{\mathrm{fII}},\ \tilde{u}_1^{\mathrm{sII}} = \tilde{u}_1^{\mathrm{gII}} \tag{37}$$

At $x_3 = H+h_w + h_{w2} + h_{w3}+h$:

$$\tilde{\sigma}_{33}^{\mathrm{II}} - \tilde{\sigma}_{33}^{\mathrm{III}} = q_0 \frac{\sin(\xi l)}{\xi l},\ \tilde{\sigma}_{13}^{\mathrm{II}} = \tilde{\sigma}_{13}^{\mathrm{III}},\ \tilde{u}_3^{\mathrm{sII}} = \tilde{u}_3^{\mathrm{sIII}},\ \tilde{u}_1^{\mathrm{sII}} = \tilde{u}_1^{\mathrm{sIII}} \tag{38}$$

Substituting Eqs. (27-32) into the boundary conditions (33-38), the following matrix equations yields:

$$[T]\{x\} = \{f\} \tag{39}$$

where the elements in matrix $[T]$ and vectors $\{x\}$ and $\{f\}$ are detailed in Appendix B.

By solving the Eqs. (39), the wave amplitudes of various types of waves in $\{x\}$ are obtained, and the stress and displacement responses at any point in the unsaturated soil and the WIB can be obtained by combining Eqs. (27-32).

## 6 Numerical examples

For unsaturated soil, due to the change of saturation lead to a change in the shear modulus in the soil (Lu et al., 2018; Xu and Wei, 2011), then the modified dynamic shear modulus is used in this paper:

$$\mu_p = \mu_s + \frac{2050}{\alpha} \ln\left[\sqrt{(S_e)^{-2} - 1} + (S_e)^{-1}\right] \tan\phi' \tag{40}$$

In order to study the effect of WIB on the vibration control of unsaturated ground, a set of physical and mechanical parameters (Xu and Wei, 2011) of unsaturated ground are selected in this paper as shown in Table 1. Taking the load amplitude is $q_0$=1kPa and the distribution length is $l$=1m. Since the complexity of the integrand function expression, it is difficult to obtain the closed-form solution of the Fourier inverse transform. In this paper, the FFT method is used to complete the Fourier inverse transform. The discrete point of the wave number is 1024, and the spatial calculation interval is 100 m.

**Table 1** Physical and mechanical parameters of unsaturated soils

| Parameter | Unit | Value of a quantity | Parameter | Unit | Value of a quantity | Parameter | Value of a quantity |
|---|---|---|---|---|---|---|---|
| $K_g$ | kPa | 100 | $K_s$ | GPa | 36 | $S_r$ | 0.1-1 |
| $\rho_g$ | kg/m$^3$ | 1.29 | $\rho_s$ | kg/m$^3$ | 0.2 | d | 2 |
| $\eta_g$ | Ns/m$^2$ | 1.5×10$^{-5}$ | ϕ’ | ◦ | 21 | $S_{w0}$ | 0.05 |
| $K_l$ | GPa | 2.1 | α | Pa$^{-1}$ | 1×10$^{-4}$ | k | 1×10$^{-12}$ |
| $\rho_l$ | kg/m$^3$ | 1000 | $\mu_s$ | MPa | 19.4 | υ | 0.2 |
| $\eta_l$ | Ns/m$^2$ | 0.001 | n | | 0.6 | m | 0.5 |

### 6.1 *Validation of the present solution*

In order to verify the correctness of the method in this paper, Eq. (39) degenerates to the case without WIB. When $H+h_{w1}+h_{w2}+h_{w3}+h=0$, the load degenerates to the surface strip harmonic load. Shi et al. (2021) studied the dynamic response of unsaturated soil foundations under strip harmonic load. Saturation is $S_r=0.8$, circular frequency is $\omega=1$rad/s, and the rest of the unsaturated soil physical and mechanical parameters are shown in Table 1. Figure 2 shows the variation curve of the vertical displacement of the surface along the horizontal direction. It can be seen from the figure that the calculation results of this paper are in good agreement with the results of Shi.

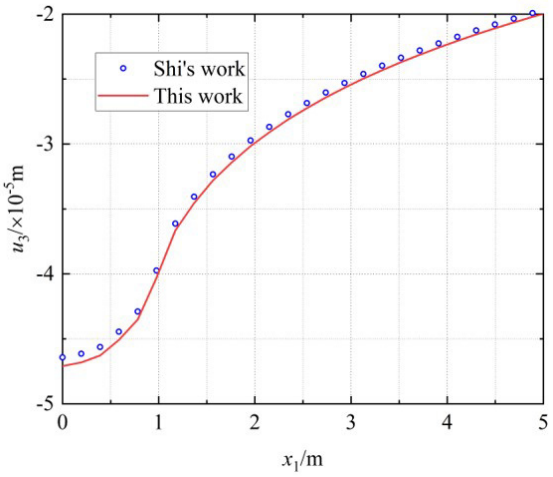


**Figure 2** Variation curve of vertical displacement of the ground surface along the horizontal direction.

In order to further verify the correctness of the method in this paper, when $S_r \to S_{w0}$, $n \to 0$, the unsaturated soil foundation degenerates into an elastic foundation. When the material parameters of the local foundation and the composite layer WIB are the same, the model in this paper degenerates into the Lamb problem where the vibration source is located in the semi-infinite homogeneous medium. Taking $\omega=0.01$rad/s, the elastic modulus of the material is $E=1\times10^7$Pa, Poisson's ratio is $v=0.3$, density is $\rho=1884$kg/m$^3$. Figure 3 shows the positive stress diagram of strip load acting on the edge of load $H+h_{w1}+h_{w2}+h_{w3}+h=4$m from the foundation surface, and compared with the analytical solution obtained by Yuan and Zhao (1995). It can be seen from Figure 3 that when the frequency is very small, it is basically consistent with the static solution.

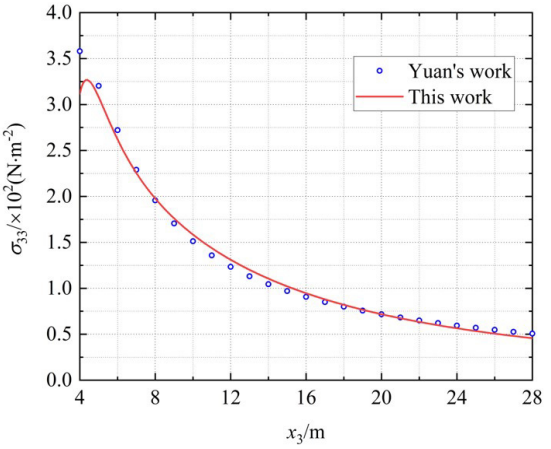


**Figure 3** The normal stress under the corner point of internal load.

### 6.2 *Example analysis*

It is known that the wave impedance (Xiang., 2011) is defined as the product of velocity and density, i.e., $Z=\rho v$. The ratio of the wave impedance of the first medium $\rho_1 v_1$ and the wave impedance of the second medium $\rho_2 v_2$ on the dividing surface of different media is the wave impedance ratio, which can be expressed as: $Z=\rho_1 v_1/\rho_2 v_2$. Let the wave impedance of unsaturated soil be $Z_0$, and the wave impedances of $WIB_1$, $WIB_2$, and

WIB$_3$ be $Z_1$, $Z_2$, and $Z_3$, respectively. Considering the saturation of soil $S_r$=0.8 and the frequency is $f$=5Hz, then the wave speed of $P_1$ wave in unsaturated soil (Xu and Wei, 2009) can be obtained as $v_{p1}$=208.15m/s, the density of unsaturated soil is $\rho = \overline{\rho}_s + \overline{\rho}_l + \overline{\rho}_g$, then the wave impedance ratio at the intersection of WIB$_1$ and the unsaturated ground is $\gamma_1 = Z_1 / Z_0 = \sqrt{\frac{\rho_{1e}E_{1e}\left(1-\upsilon_{1e}\right)}{(1+\upsilon_{1e})(1-2\upsilon_{1e})}} / \rho v_{p1}$, the wave impedance ratio at the intersection of WIB$_2$ and WIB$_1$ layers is $\gamma_2 = Z_2 / Z_1 = \sqrt{\frac{\rho_{2e}E_{2e}\left(1-\upsilon_{2e}\right)(1+\upsilon_{1e})(1-2\upsilon_{1e})}{\rho_{1e}E_{1e}(1-\upsilon_{1e})(1+\upsilon_{2e})(1-2\upsilon_{2e})}}$, the wave impedance ratio at the intersection of WIB$_3$ and WIB$_2$ layers is $\gamma_3 = Z_3 / Z_2 = \sqrt{\frac{\rho_{3e}E_{3e}\left(1-\upsilon_{3e}\right)(1+\upsilon_{2e})(1-2\upsilon_{2e})}{\rho_{2e}E_{2e}(1-\upsilon_{2e})(1+\upsilon_{3e})(1-2\upsilon_{3e})}}$.

The greater the difference at the interface of the media intersection the more significant the amplitude attenuation of the elastic wave, so the greater the difference in wave impedance at the interface, the more significant the amplitude attenuation of the elastic wave. From the definition of wave impedance, it can be seen that the material parameters affecting the medium wave impedance are mainly density and elastic modulus. Therefore, this paper by analyzing the influence of the wave impedance ratio at the interface between the composite multilayer WIB and the unsaturated ground layer on the vibration isolation performance of the composite multilayer WIB, the corresponding interlayer wave impedance ratio with the best vibration isolation effect is selected, and then back calculates the elastic modulus and density of the interlayer material of the composite multilayer WIB, and finally obtains the design guidelines of the interlayer material parameters of the composite multilayer WIB. The physical and mechanical parameters of the composite multilayer WIB are selected as follows: Poisson's ratio is $\upsilon_{1e}$=$\upsilon_{2e}$=$\upsilon_{3e}$=0.3, the thickness of the composite multilayer WIB is $h_{w1}$=$h_{w2}$=$h_{w3}$=0.5m respectively, and the density of the composite multilayer WIB is discussed in the following six cases:

Case1: $\rho_{1e}$=$3700kg/m^3 > \rho_{2e}$=$2700kg/m^3 > \rho_{3e}$=$1700kg/m^3$

Case2: $\rho_{1e}$=$3700kg/m^3 > \rho_{3e}$=$2700kg/m^3 > \rho_{2e}$=$1700kg/m^3$

Case3: $\rho_{2e}$=$3700kg/m^3 > \rho_{1e}$=$2700kg/m^3 > \rho_{3e}$=$1700kg/m^3$

Case4: $\rho_{2e}$=$3700kg/m^3 > \rho_{3e}$=$2700kg/m^3 > \rho_{1e}$=$1700kg/m^3$

Case5: $\rho_{3e}$=$3700kg/m^3 > \rho_{1e}$=$2700kg/m^3 > \rho_{2e}$=$1700kg/m^3$

Case6: $\rho_{3e}$=$3700kg/m^3 > \rho_{2e}$=$2700kg/m^3 > \rho_{1e}$=$1700kg/m^3$

Considering the soil saturation of $S_r$=0.8, the load frequency of $f$=5Hz, the embedded depth of WIB is $H$=1m, and the distance of the vibration source from WIB is $h$=3-$H$-$h_{w1}$-$h_{w2}$-$h_{w3}$. Figure 4 gives the four-dimensional plots of the simultaneous variation of the surface vertical displacement maxima with the wave impedance ratios $\gamma_1$, $\gamma_2$, and $\gamma_3$ under an underground dynamic load in six cases, respectively, with the independent variables being the wave impedance ratios $\gamma_1$, $\gamma_2$, and $\gamma_3$, and the stress variable being the surface vertical displacement maxima $|u_3|_{max}$, and the color changes represent the variation of the surface vertical displacement maxima. By comparing the minimum value of the maximum value of the vertical displacement of the ground under the simultaneous change of the interlayer wave impedance ratio, the value of the interlayer wave impedance ratio of the composite multilayer WIB with the best vibration isolation effect can be selected. From Figure 4(a~f), it can be seen that when the wave impedance ratio is small, with the increase of the wave impedance ratio, the maximum value of vertical displacement of the ground surface decreases sharply, but when the wave impedance ratio increases to a certain degree, the maximum value of vertical displacement of the surface reaches the minimum. In the range of the wave impedance ratio discussed in this paper, there is the interlayer wave impedance ratio that corresponds to the maximum value of vertical displacement of the ground surface when it reaches the minimum, which is the best vibration isolation effect of the composite multilayer WIB. From Figure 4(a~f), we can get the interlayer wave impedance ratio corresponding to the optimum vibration isolation effect of composite multilayer WIB in six cases, i.e., when the maximum value of vertical displacement of the ground surface reaches the minimum, respectively:

Case1: $\gamma_1$ =4.5, $\gamma_2$ =20.5, $\gamma_3$ =0.5, $|u_3|_{max}$=1.22×10$^{-8}$m

Case2: $\gamma_1$ =4.5, $\gamma_2$ =16.5, $\gamma_3$ =1.0, $|u_3|_{max}$=1.08×10$^{-8}$m

Case3: $\gamma_1$ =4.5, $\gamma_2$ =22.0, $\gamma_3$ =0.5, $|u_3|_{max}$=1.44×10$^{-8}$m

Case4: $\gamma_1$ =4.0, $\gamma_2$ =21.5, $\gamma_3$ =0.5, $|u_3|_{max}$=2.38×10$^{-8}$m

Case5: $\gamma_1$ =3.5, $\gamma_2$ =21.0, $\gamma_3$ =1.0, $|u_3|_{max}$=1.38×10$^{-8}$m

Case6: $\gamma_1$ =3.5, $\gamma_2$ =22.0, $\gamma_3$ =1.0, $|u_3|_{max}$=1.82×10$^{-8}$m

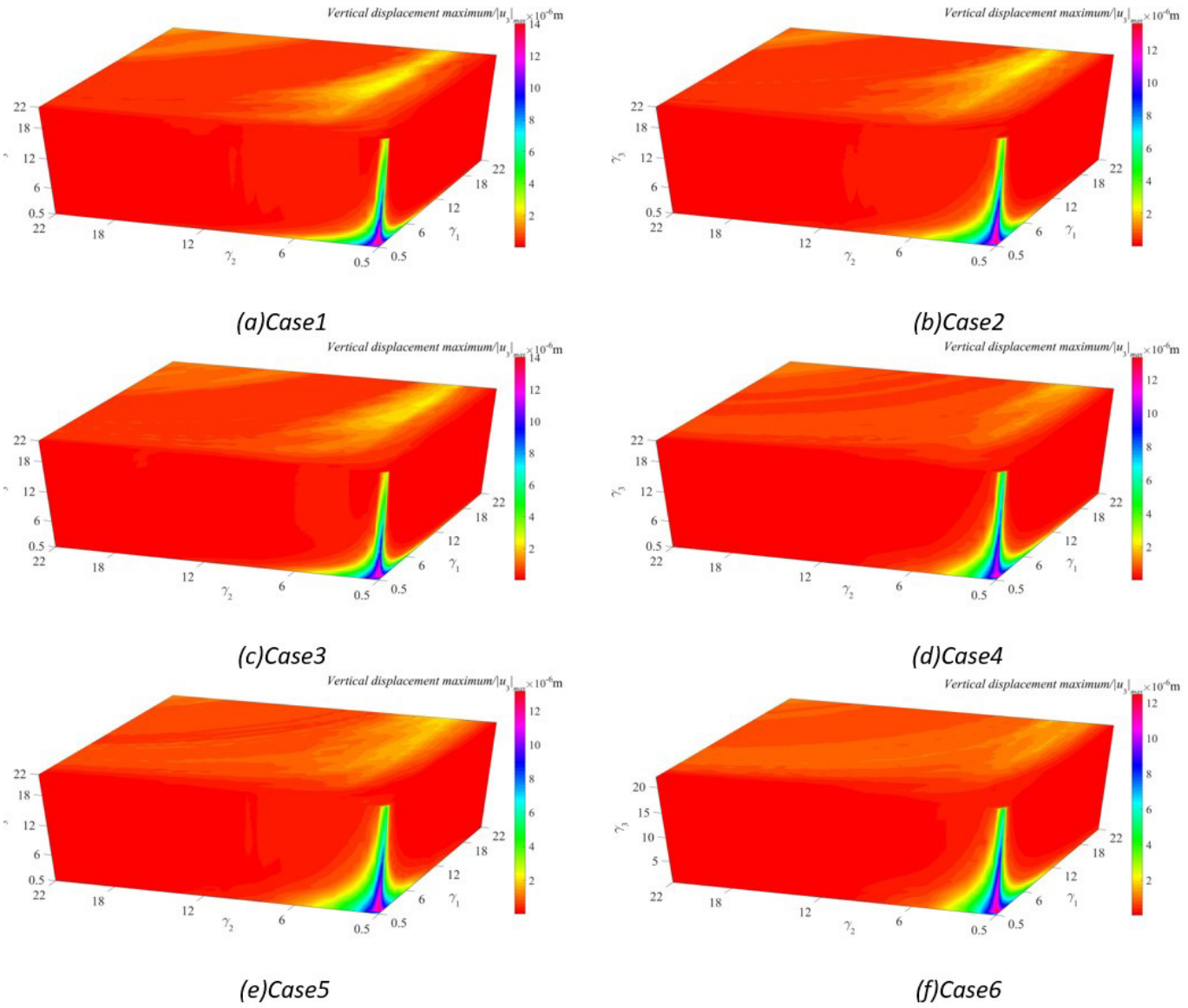


**Figure 4** Four-dimensional plot of the variation of the vertical displacement maximum of the ground surface with the wave impedance ratio.

From the above six cases and in the range of wave impedance ratio considered in this paper, it can be seen that when the density case is Case2, the composite multilayer WIB can achieve the optimal vibration isolation effect. At this time, the elastic modulus of the composite multilayer WIB is $E_{1e}$=4.62×10$^8$Pa, $E_{2e}$=2.74×10$^{11}$Pa, and $E_{3e}$=1.72×10$^{11}$Pa. Therefore, the optimal vibration isolation effect of the composite multilayer WIB can be obtained by designing the wave impedance ratio between the layers of the composite multilayer WIB. In addition, due to the transmission effect of the barrier, directly affects the vibration isolation efficiency (Gao et al., 2021), when the impedance of the barrier is relatively large, it can reduce the transmission of vibration waves from the soil surface, and the larger the impedance ratio is the

better vibration isolation efficiency can be obtained. However, it is obviously unrealistic to take the infinite wave impedance ratio in practical engineering. Therefore, the composite multilayer WIB vibration isolation barrier system proposed in this paper is superior and designable.

In the following analysis and comparison, the density corresponding to Case2 and the inter-layer wave impedance ratio corresponding to the optimal isolation effect of the composite multilayer WIB is taken to analyze the vibration isolation performance law of the composite multilayer WIB.

In order to compare the advantages and disadvantages of the vibration isolation effect of composite multilayer WIB and homogeneous WIB under the same conditions, consider the embedded depth of WIB is $H$ =1m, the soil saturation is $S_r$=0.8, the load frequency is $f$=5Hz, the distance of vibration source from WIB is $h$=3-$H$-$h_{w1}$-$h_{w2}$-$h_{w3}$m, the Poisson's ratio of composite multilayer WIB and homogeneous WIB are $\upsilon_{1e}$=$\upsilon_{2e}$=$\upsilon_{3e}$=0.3, the thickness of composite multilayer WIB are $h_{w1}$=$h_{w2}$=$h_{w3}$=0.5m , the thickness of the homogeneous WIB is $h_w$=1.5m, the density of the composite multilayer WIB are $\rho_{1e}$=3700kg/m$^3$, $\rho_{2e}$=1700kg/m$^3$, $\rho_{3e}$=2700kg/m$^3$, the elastic modulus of the composite multilayer WIB are $E_{1e}$=4.62×10$^8$Pa, $E_{2e}$=2.74×10$^{11}$Pa, $E_{3e}$=1.72×10$^{11}$Pa. Because the vibration isolation effect of the homogeneous WIB increases with the increase of elastic modulus (Gao and Li, 2005; Gao et al., 2007), in order to compare the vibration isolation effect of the composite multilayer WIB and the homogeneous WIB, the density and elastic modulus of the homogeneous WIB are taken as their maximum values, namely: $\rho_e$=3700kg/m$^3$, $E_e$=2.74×10$^{11}$Pa. For the evaluation of the vibration isolation effect of the composite multilayer WIB, the amplitude attenuation coefficient $A_R$ proposed by Woods (1968) is used to measure :

$$A_R = \frac{\overline{u}}{u} \tag{41}$$

where $\overline{u}$ is the surface displacement after setting the WIB barrier, and $u$ is the surface displacement without the WIB barrier.

Figure 5 plots the change curve of the amplitude attenuation coefficient of the vertical displacement of the ground surface with the distance when the composite multilayer WIB and homogeneous WIB are installed in the unsaturated ground. According to Figure 5, it can be seen that the surface vertical displacement amplitude attenuation coefficient of the composite multilayer WIB is significantly smaller than that of the homogeneous WIB, and the corresponding surface vertical displacement amplitude attenuation coefficient of the composite multilayer WIB is much smaller than 1. Therefore, under the same conditions, the design of composite multilayer WIB compared to homogeneous WIB can not only reduce the use of high-strength materials, and improve the vibration isolation performance, composite multilayer WIB than homogeneous WIB has a superior vibration isolation effect.

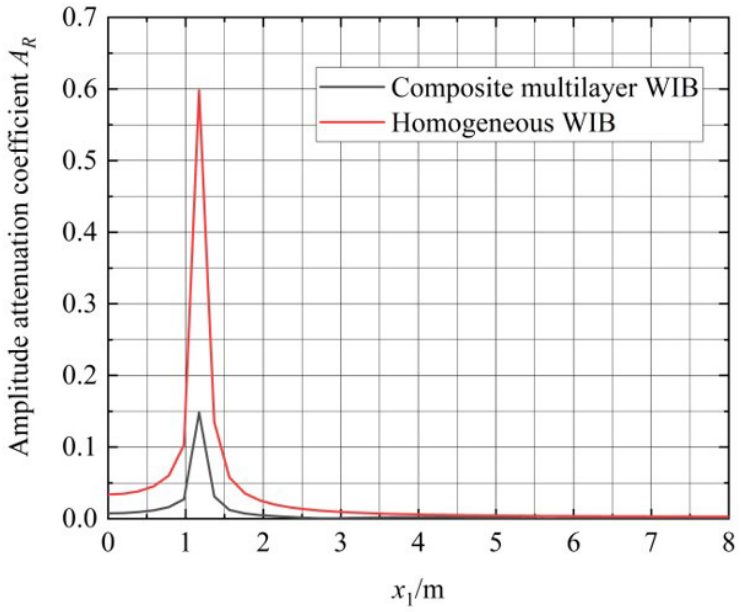


**Figure 5** Variation curve of amplitude attenuation coefficient $A_R$ of the ground surface with distance for vertical displacement.

In order to analyze the effect of the saturation of the soil on the vibration isolation effect of the composite multilayer WIB, Figure 6 plots the change curve of the amplitude attenuation coefficient of the vertical displacement of the ground surface with the distance when the saturation increases gradually from $S_r$=0.3, 0.5, 0.7, 0.8, 0.9 at $H$=1m, $h_{w1}$=$h_{w2}$=$h_{w3}$=0.5m, $f$=5Hz, $h$=3-$H$-$h_{w1}$-$h_{w2}$- $h_{w3}$m. It can be seen from Figure 6 that the amplitude attenuation coefficient of vertical displacement of the ground surface increases with the increase of the saturation degree, which indicates that the vibration isolation effect of the composite multilayer WIB is decreasing with the increase of the saturation degree. When $S_r$=0.9, the surface vertical displacement amplitude attenuation coefficient increases sharply, and the value is greater than 1, indicating that the vibration isolation failure occurs at this time. When $S_r$≤0.8, the surface vertical displacement amplitude attenuation coefficient is much less than 1, which indicates that the composite multilayer WIB can play a good vibration isolation effect in the unsaturated ground in the range of $S_r$≤0.8. From the perspective of the vibration isolation mechanism of the wave impeding block, the good vibration isolation performance of the wave impeding block is mainly due to its reflection and scattering of waves (Song et al., 2022). When the saturation of the unsaturated soil foundation is less than 0.8, the total compression modulus of the soil is controlled by the soil skeleton. When the saturation increases to 0.9, the gas phase in the soil decreases, the liquid phase increases, and the equivalent compression modulus of the pore fluid increases rapidly. The total compression modulus of the soil is controlled by the compression modulus of the soil skeleton and the equivalent compression modulus of the pore fluid, which makes the longitudinal wave velocity in the foundation increase rapidly under the action of underground dynamic load, which leads to the increase of the saturation of unsaturated foundation. The complex change of the vertical displacement amplitude attenuation coefficient of the wave impeding block. Therefore, the saturation of the site soil has a significant effect on the vibration isolation effect of the WIB, which indicates that the design of vibration isolation of WIB in actual engineering should choose a ground model that matches the actual site, and simplify the site soil as a single-phase elastic ground or a saturated ground without considering the effect of the saturation of the soil on the vibration isolation effect, which is very different from the actual phenomenon. It can be seen from Figure 6 that it is desirable to set the composite multilayer WIB in the range of $S_r$≤0.8 in the unsaturated ground to obtain the ideal vibration isolation effect.

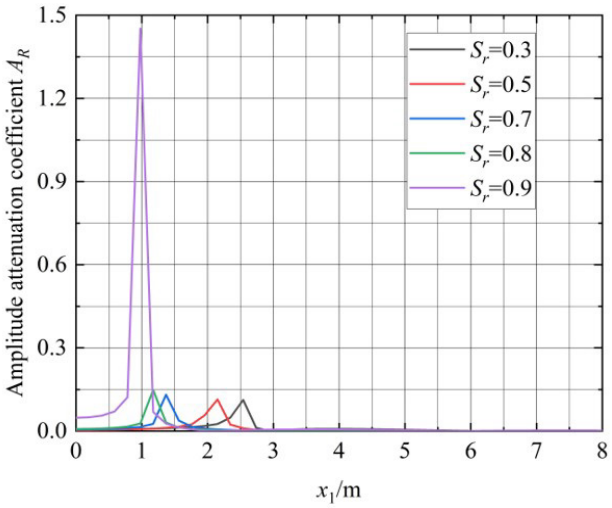


**Figure 6** Variation curve of amplitude attenuation coefficient $A_R$ of the ground surface under different saturation with distance for vertical displacement.

In order to analyze the effect of load frequency on the vibration isolation effect of the composite multilayer WIB, Figure 7 shows the change curve of the amplitude attenuation coefficient of the vertical displacement of the ground surface with the distance when the load frequency increases gradually from $f$=5, 20, 40, 80, 100, and 120 Hz at $H$=1m, $S_r$=0.8, $h_{w1}$=$h_{w2}$=$h_{w3}$=0.5m, and $h$=3-$H$-$h_{w1}$-$h_{w2}$-$h_{w3}$m. It can be seen from Figure 7 that when the load frequency $f$ ≤20Hz, with the increase of load frequency, the attenuation coefficient of surface vertical displacement amplitude decreases, and the vibration isolation effect of composite multilayer WIB is gradually enhanced. When the load frequency is in the range of 20Hz≤$f$≤100Hz, with the increase of load frequency, the surface vertical displacement amplitude attenuation coefficient increases, and the surface vertical displacement amplitude attenuation coefficient is less than1, only when $f$ = 120Hz, the corresponding surface vertical displacement attenuation coefficient is greater than1. In summary, the composite multilayer WIB has a good damping effect on the high-frequency vibration in the load frequency range of 5Hz≤$f$≤100Hz. In contrast, the traditional homogeneous WIB only has a good vibration isolation effect on low-frequency

vibration, and there is a phenomenon of far-field amplification failure in the vibration isolation of medium and high-frequency vibration. The composite multilayer WIB vibration isolation barrier proposed in this paper improves the frequency width of the homogeneous WIB vibration isolation. The composite multilayer WIB also has a good vibration isolation effect on low, medium, and high-frequency vibration (5Hz≤$f$≤100Hz), which again illustrates the superiority of the composite multilayer WIB vibration isolation system.

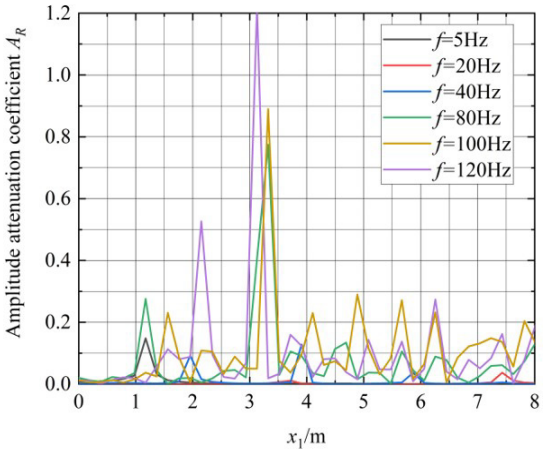


**Figure 7** Variation curve of amplitude attenuation coefficient $A_R$ of the ground surface under different loading frequencies with distance for vertical displacement.

In order to analyze the effect of the thickness of the composite multilayer WIB on the vibration isolation effect of the ground, Figure 8 plots the variation curve of the amplitude attenuation coefficient of the surface vertical displacement with distance when the thickness of the WIB increases gradually from $h_{w1}$=$h_{w2}$=$h_{w3}$=0.3, 0.4, 0.5, 0.6m at $H$=1m, $S_r$=0.8, $f$=5Hz, $h$=3-$H$-$h_{w1}$-$h_{w2}$-$h_{w3}$m. From Figure 8, it can be seen that when 0.3m≤$h_{w1}$=$h_{w2}$=$h_{w3}$≤0.5m, the attenuation coefficient of vertical displacement amplitude decreases with the increase of the thickness of the WIB, indicating that the vibration isolation effect of the composite multilayer WIB is gradually enhanced. When the thickness of the WIB $h_{w1}$=$h_{w2}$=$h_{w3}$ ≥0.5m, the attenuation coefficient of the vertical displacement amplitude increases with the increase of the thickness of the WIB, indicating that the vibration isolation effect is no longer obvious when the thickness of the WIB continues to increase, and the composite multilayer WIB has a critical thickness. This phenomenon is consistent with the law of the WIB-Duxseal joint vibration isolation test study (Tian et al., 2020, Gao et al., 2021 ) on the effect of thickness under vertical excitation force. Therefore, when designing the vibration isolation of composite multilayer WIB in practical engineering, the thickness of composite multilayer WIB should not be set too thick considering the appropriate economic cost and better vibration isolation effect. From Figure 8, it can be seen that the thickness of the composite multilayer WIB should be $h_{w1}$=$h_{w2}$=$h_{w3}$=0.5m, which can play a better vibration control effect in unsaturated soil foundations.

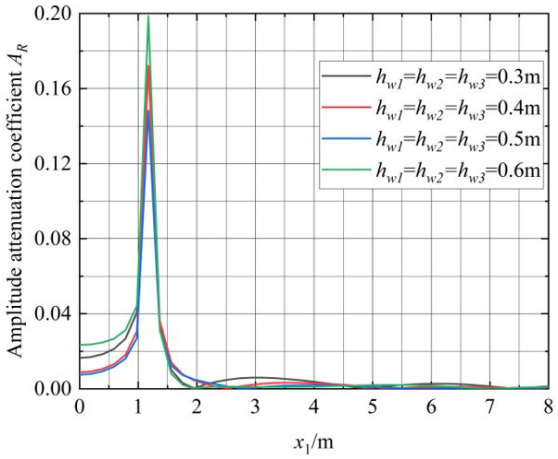


**Figure 8** Variation curve of amplitude attenuation coefficient $A_R$ of the ground surface under different thicknesses with distance for vertical displacement.

In order to analyze the effect of the embedded depth of the composite multilayer WIB on the vibration isolation effect of the ground, Figure 9 plots the variation curve of the amplitude attenuation coefficient of the surface vertical displacement with distance when the embedded depth of the WIB increases gradually from $H$=1, 2, 3m at $h_{w1}$=$h_{w2}$=$h_{w3}$=0.5m, $S_r$=0.8, $f$=5Hz, $h$=5.5-$H$-$h_{w1}$-$h_{w2}$-$h_{w3}$m. It can be seen from Figure 9 that when the embedded depth is larger, the attenuation coefficient of the vertical displacement amplitude of the surface is smaller, that is, when the WIB is closer to the vibration source, the vibration isolation effect is better. This is because the WIB uses the principle of the cut-off frequency of the foundation to isolate the vibration. Only when the WIB is close to the vibration source, even if there is an effective cut-off frequency of the foundation, can the vibration isolation effect on the environmental vibration be achieved. Therefore, when the position of the WIB is set, the composite multilayer WIB is set closer to the vibration source so that there is an effective cut-off frequency in the foundation, and the vibration isolation effect of the WIB is better.

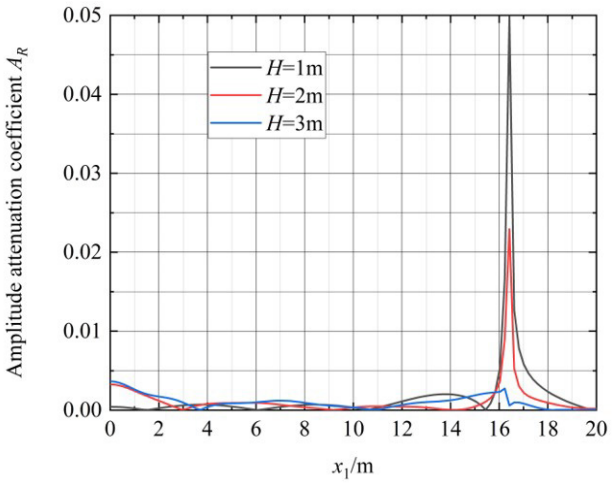


**Figure 9** Variation curve of amplitude attenuation coefficient $A_R$ of the ground surface under different embedded depths with distance for vertical displacement.

## 7 Conclusions

Based on single-phase elastic medium theory and unsaturated porous medium theory, the vibration isolation performance of composite multilayer WIB vibration isolation system in the unsaturated ground under an underground dynamic load is studied in this paper, and the advantages and disadvantages of the vibration isolation effect of composite multilayer WIB and homogeneous WIB under the same conditions are compared. The influence of soil saturation, load frequency, thickness, and embedded depth of the WIB on the vibration isolation performance of composite multilayer WIB was analyzed. The results of the study show that:

(1) The effect of the interlayer wave impedance ratio of composite multilayer WIB and unsaturated soil foundation on the vibration isolation effect of composite multilayer WIB is very obvious. By designing the wave impedance ratio between the composite multilayer WIB and the unsaturated soil foundation, the optimal vibration isolation effect of the composite multilayer WIB vibration isolation barrier can be obtained.

(2) Under the same thickness condition, the vibration isolation effect of the designed composite multilayer WIB is much better than that of the homogeneous WIB. Compared with the homogeneous WIB, the composite multilayer WIB improves the vibration isolation bandwidth and has a good vibration isolation effect in the range of 5≤$f$≤100 Hz.

(3) The soil saturation has a significant influence on the vibration isolation effect of the composite multilayer WIB, and the composite multilayer WIB can have a good vibration isolation effect in the range of $S_r$≤0.8. The foundation model that is consistent with the actual site should be selected in the design of WIB vibration isolation in practical engineering.

(4) The closer the embedded depth of the composite multilayer WIB is to the vibration source, the better the vibration isolation effect is. There is a critical thickness of the composite multilayer WIB. When the thickness of the WIB exceeds the critical thickness, the vibration isolation effect of the WIB decreases with the increase of thickness.

## Acknowledgments

The authors gratefully acknowledge the financial support of the Chinese Natural Science Foundation (Grant No. 52168053), the authors are also grateful to the reviewers for their helpful advice and comments.

**Author's Contributions:** Conceptualization, Meng Zhang and Qiang Ma; Methodology, Meng Zhang and Qiang Ma; Investigation, Qiang Ma; Writing - original draft, Meng Zhang; Writing - review & editing, Meng Zhang and Qiang Ma; Resources, Meng Zhang and Qiang Ma; Supervision, Qiang Ma.

**Editor**: Pablo Andrés Muñoz Rojas

## References

Ba, Z.N., Liu, S.P., Wu, M.T., et al. (2022). Analytical solution for isolation effect of plane SH waves by periodically distributed piles. Rock Soil Mech 41(09), 2861-2868.

Chouw, N., Le, R., Schmid, G. (1991). An approach to reduce foundation vibrations and soil waves using dynamic transmitting behavior of a soil layer. Bauingenieur 66, 215-221.

Gao, G.Y., Chen, J., Gu, X.Q., et al. (2017). Numerical study on the active vibration isolation by WIB in saturated soils under vertical loading. Soil Dyn Earthq Eng 93, 99-112.

Gao, G.Y., Feng, S.J., Li, W., et al. (2007). 2-D analysis of vibration isolation by WIB in layered ground. J Vib Eng, (02), 174-179.

Gao, GY., Li, W. 2005 2-D analysis of ground vibration isolation using WIB. Earthq Eng Eng Dyn (02), 130-135.

Gao, G.Y., Wang, F., Chen, G.Q. (2014). Active vibration isolation of the saturated ground with WIB inside and under the load of the travelling train. J Vib Eng 27(03), 433-440.

Gao, G.Y., Zhang, Q.W., Chen, J., et al. (2018) Field experiments and numerical analysis on the ground vibration isolation of WIB under horizontal and rocking coupled excitations. Soil Dyn Earthq Eng 115, 507-512.

Gao, GY. (1998) Theory and Application of Ground Vibration Isolation by Discontinuous Barrier, Ph.D. Thesis (in Chinese), Zhejiang University, China.

Gao, M., Tian, S.P., Wang, Y., et al. (2020). Isolation of ground vibration induced by high speed railway by DXWIB: Field investigation. Soil Dyn Earthq Eng 131, 106039.

Gao, M., Zhang, Z.S., Wang, C.G., et al. (2021). Field test on vibration isolation performance by WIB-Duxseal under vertical excitation. Rock Soil Mech 42(02), 537-546.

Huang. L., Liu, Z., Wu. C., et al. (2022). A three-dimensional indirect boundary integral equation method for the scattering of seismic waves in a poroelastic layered half-space. Eng Anal Bound Elem 135, 167-181.

Li, Y., Di, H., Zhou, S., et al. (2021). Seismic analysis for cross transfer subway stations in soft soil stratum. KSCE J Civ Eng 25(05), 1732-1745.

Liu, Z.X., Fu, Z.Y., Miao, Y., et al. (2019). 3D simulation for broadband scattering of rayleigh wave by discontinuous barrier based on FMP-IBEM. J Vib Shock 38(19), 89-97.

Lu, Z., Fang, R., Yao, H., et al. (2018). Dynamic responses of unsaturated half-space soil to a moving harmonic rectangular load. Int J Numer Anal Methods Geomech 42(09), 1057-1077.

Ma, Q., Zhou, F.X., Liu, J. (2017). Analysis of ground vibration control by graded WIB. J Chin J Theor Appl 49(06), 1360-1369.

Ma, Q., Zhou, F.X., Zhang, W.Y. (2019). Vibration isolation of saturated foundations by functionally graded WIB under a moving load. J Braz Soc Mech Sci Eng 41(02), 108.

Ma, Q. 2018 Study on isolation barrier based on gradient non-homogeneous WIB, Ph.D. Thesis (in Chinese), Lanzhou University of Technology, China.

Schevenels, M., Lombaert, G. (2017). Double wall barriers for the reduction of ground vibration transmission. Soil Dyn Earthq Eng 97, 1-13.

Shi, L.W., Ma, Q., Ma, Y.X. (2021). Dynamic responses of unsaturated half-space soils to a strip load at different boundary conditions. Arab J Geosci 14(11), 1-11.

Shu, J.H., Ma, Q., Zhou, F.X., et al. (2022). Study on the propagation characteristics of P1 wave passing through WIB in unsaturated soil. Rock Soil Mech., 43(04), 1-13.

Song Y.S., Gao, M., Chen, Q.S. (2022). Study on the isolation performance of WIB on nearly-saturated ground under moving load. Earthq Eng Eng Dyn 42(02), 252-263.

Takemiya, H., Fujiwara, A. (1994). Wave propagation / impediment in a stratum and WIB (WIB) measured for SSI response reduction. Soil Dyn Earthq Eng 13(01), 49-61.

Tian, S.P, Gao, M., Wang, Y., et al. (2020). Numerical analysis and field experiment on vibration isolation for Duxseal. Rock Soil Mech 42(05), 1770-1780.

Woods, R.D. (1968). Screening of surface waves in soils. J Soil Mech Found Div 94(04), 951-979.

Xiang, G.W. (2011). Numerical and experimental study on vibration isolation measures with barriers, Ph.D. Thesis (in Chinese), Shanghai Jiao Tong university, China.

Xu, M.J., Wei, D.M. (2011). 3D non-axisymmetric dynamic response of unsaturated soils. J Eng Mech 28(03), 78-85.

Xu, M.J., Wei, D.M. (2009). Characteristics of wave propagation in partially saturated poroelastic media. Sci Tech Eng (18), 5403-5409.

Xu, P., Zhou, F.X., Xia, T.D. (2015). Review on passive vibration isolation using barriers. J China Earthq Eng 37(01), 88-93.

Yuan, J.Y., Zhao, X.H. (1995). Formulas for the calculation of stresses in soil subjecting to distributed loading beneath the surface of the ground. Shanghai Mech 16(3), 213-222.

Zhou, F.X., Cao, Y.C., Zhao, W.G. (2015). Analysis of dynamic response of inhomogeneous subgrade under moving loads. Rock Soil Mech 36(07), 2027-2033.

Zhou, F.X., Ma, Q., Zhou, Z.X. (2020). 2D analysis of vibration-isolation efficiency of an open trench-wave impedence block barrier. Rock Soil Mech 41(12), 4087-4092+4115.

Zienkiewicz, O.C., Chang, C.T., Beetts, P. (1980). Drained, undrained, consolidating and dynamic behavior assumptions in soils. Geotechnqiue 30(04), 385-395.

## Appendix A - The coefficient of the root of the potential function

$$\beta_1 = -B_1a_{12}a_{23} + B_1a_{13}a_{22} + B_2a_{11}a_{23} - B_2a_{13}a_{21} - B_3a_{11}a_{22} + B_3a_{12}a_{21} - \mu_p a_{12}a_{23} + \mu_p a_{13}a_{22}$$

$$\beta_2 = -B_1a_{12}b_{33} + B_1a_{13}b_{32} + B_1a_{22}b_{23} - B_1a_{23}b_{22} + B_2a_{11}b_{33} - B_2a_{13}b_{31} - B_2a_{21}b_{23} + B_2a_{23}b_{21} - B_3a_{11}b_{32} + B_3a_{12}b_{31} + B_3a_{21}b_{22} - B_3a_{22}b_{21} - a_{11}a_{22}b_{13} + a_{11}a_{23}b_{12} + a_{12}a_{21}b_{13} - a_{12}a_{23}b_{11} - a_{13}a_{21}b_{12} + a_{13}a_{22}b_{11} - \mu_p a_{12}b_{33} + \mu_p a_{13}b_{32} + \mu_p a_{22}b_{23} - \mu_p a_{23}b_{22}$$

$$\beta_3 = -B_1b_{22}b_{33} + B_1b_{23}b_{32} + B_2b_{21}b_{33} - B_2b_{23}b_{31} - B_3b_{21}b_{32} + B_3b_{22}b_{31} + a_{11}b_{12}b_{33} - a_{11}b_{13}b_{32} - a_{12}b_{11}b_{33} + a_{12}b_{13}b_{31} + a_{13}b_{11}b_{32} - a_{13}b_{12}b_{31} - a_{21}b_{12}b_{23} + a_{21}b_{13}b_{22} + a_{22}b_{11}b_{23} - a_{22}b_{13}b_{21} - a_{23}b_{11}b_{22} + a_{23}b_{12}b_{21} - \mu_p b_{22}b_{33} + \mu_p b_{23}b_{32}$$

$$\beta_4 = -b_{11}b_{22}b_{33} + b_{11}b_{23}b_{32} + b_{12}b_{21}b_{33} - b_{12}b_{23}b_{31} - b_{13}b_{21}b_{32} + b_{13}b_{22}b_{31}$$

$$\beta_5 = -\mu_p d_{22}d_{33}, \beta_6 = -d_{11}d_{22}d_{33} + d_{21}d_{12}d_{33} + d_{13}d_{22}d_{31}$$

## Appendix B - Specific representations of the wave amplitude coefficient matrix

The expression of the system of Eqs. (39) are as follows:

$$
\begin{aligned}
&T_{32\times32}[A_{tp1}^{\mathrm{I}} \quad A_{tp2}^{\mathrm{I}} \quad A_{tp3}^{\mathrm{I}} \quad A_{rp1}^{\mathrm{I}} \quad A_{rp2}^{\mathrm{I}} \quad A_{rp3}^{\mathrm{I}} \quad B_{ts}^{\mathrm{I}} \quad B_{rs}^{\mathrm{I}} \quad A_{1te} \quad A_{1re} \quad B_{1te} \quad B_{1re} \quad A_{2te} \quad A_{2re} \quad B_{2te} \quad B_{2re}\\
&A_{3te} \quad A_{3re} \quad B_{3te} \quad B_{3re} \quad A_{tp1}^{\mathrm{II}} \quad A_{tp2}^{\mathrm{II}} \quad A_{tp3}^{\mathrm{II}} \quad A_{rp1}^{\mathrm{II}} \quad A_{rp2}^{\mathrm{II}} \quad A_{rp3}^{\mathrm{II}} \quad B_{ts}^{\mathrm{II}} \quad B_{rs}^{\mathrm{II}} \quad A_{tp1}^{\mathrm{III}} \quad A_{tp2}^{\mathrm{III}} \quad A_{tp3}^{\mathrm{III}} \quad B_{ts}^{\mathrm{III}}]^{\mathrm{T}} =\\
&[0 \quad 0 \quad 0 \quad 0 \quad 0 \quad 0 \quad 0 \quad 0 \quad 0 \quad 0 \quad 0 \quad 0 \quad 0 \quad 0 \quad 0 \quad 0 \quad 0 \quad 0 \quad 0 \quad 0 \quad 0 \quad 0 \quad 0 \quad 0 \quad 0 \quad 0\\
&q_0 \frac{\sin(\xi l)}{\xi l} \quad 0 \quad 0 \quad 0]^{\mathrm{T}}
\end{aligned}
$$

The elements not 0 in matrix T are as follows:

$$
\begin{aligned}
&T_{0101} = T_{0104} = \chi_1, T_{0102} = T_{0105} = \chi_2, T_{0103} = T_{0106} = \chi_3, T_{0107} = -2\mu_p \mathrm{i}\xi r, T_{0108} = 2\mu_p \mathrm{i}\xi r, T_{0201} = -2\mu_p \mathrm{i}\xi\lambda_1,\\
&T_{0202} = -2\mu_p \mathrm{i}\xi\lambda_2, T_{0203} = -2\mu_p \mathrm{i}\xi\lambda_3, T_{0204} = 2\mu_p \mathrm{i}\xi\lambda_1, T_{0205} = 2\mu_p \mathrm{i}\xi\lambda_2, T_{0206} = 2\mu_p \mathrm{i}\xi\lambda_3,\\
&T_{0207} = T_{0208} = -\mu_p(r^2+\xi^2), T_{0301} = T_{0304} = \left(a_{11} + a_{12}\delta_{p1}^l + a_{13}\delta_{p1}^g\right)(\xi^2 - \lambda_1^2),\\
&T_{0302} = T_{0305} = \left(a_{11} + a_{12}\delta_{p2}^l + a_{13}\delta_{p2}^g\right)(\xi^2 - \lambda_2^2), T_{0303} = T_{0306} = \left(a_{11} + a_{12}\delta_{p3}^l + a_{13}\delta_{p3}^g\right)(\xi^2 - \lambda_3^2),\\
&T_{0401} = T_{0304} = \left(a_{21} + a_{22}\delta_{p1}^l + a_{23}\delta_{p1}^g\right)(\xi^2 - \lambda_1^2), T_{0402} = T_{0405} = \left(a_{21} + a_{22}\delta_{p2}^l + a_{23}\delta_{p2}^g\right)(\xi^2 - \lambda_2^2),\\
&T_{0403} = T_{0406} = \left(a_{21} + a_{22}\delta_{p3}^l + a_{23}\delta_{p3}^g\right)(\xi^2 - \lambda_3^2), T_{0501} = \chi_1 \mathrm{e}^{-\lambda_1 H}, T_{0502} = \chi_2 \mathrm{e}^{-\lambda_2 H}, T_{0503} = \chi_3 \mathrm{e}^{-\lambda_3 H}, T_{0504} = \chi_1 \mathrm{e}^{\lambda_1 H},\\
&T_{0505} = \chi_2 \mathrm{e}^{\lambda_2 H}, T_{0506} = \chi_3 \mathrm{e}^{\lambda_3 H}, T_{0507} = -2\mu_p \mathrm{i}\xi r \mathrm{e}^{-rH}, T_{0508} = 2\mu_p \mathrm{i}\xi r \mathrm{e}^{rH}, T_{0509} = \left[\lambda_{1e}\xi^2 + \alpha_{1e}^2(\lambda_{1e} + 2\mu_{1e})\right]\mathrm{e}^{-\mathrm{i}\alpha_{1e}H},\\
&T_{0510} = \left[\lambda_{1e}\xi^2 + \alpha_{1e}^2(\lambda_{1e} + 2\mu_{1e})\right]\mathrm{e}^{\mathrm{i}\alpha_{1e}H}, T_{0511} = -2\mu_{1e}\xi\beta_{1e}\mathrm{e}^{-\mathrm{i}\beta_{1e}H}, T_{0512} = 2\mu_{1e}\xi\beta_{1e}\mathrm{e}^{\mathrm{i}\beta_{1e}H}, T_{0601} = -2\mu_p \mathrm{i}\xi\lambda_1 \mathrm{e}^{-\lambda_1 H},\\
&T_{0602} = -2\mu_p \mathrm{i}\xi\lambda_2 \mathrm{e}^{-\lambda_2 H}, T_{0603} = -2\mu_p \mathrm{i}\xi\lambda_3 \mathrm{e}^{-\lambda_3 H}, T_{0604} = 2\mu_p \mathrm{i}\xi\lambda_1 \mathrm{e}^{\lambda_1 H}, T_{0605} = 2\mu_p \mathrm{i}\xi\lambda_2 \mathrm{e}^{\lambda_2 H}, T_{0606} = 2\mu_p \mathrm{i}\xi\lambda_3 \mathrm{e}^{\lambda_3 H},\\
&T_{0607} = -\mu_p(r^2+\xi^2)\mathrm{e}^{-rH}, T_{0608} = -\mu_p(r^2+\xi^2)\mathrm{e}^{rH}, T_{0609} = -2\mu_{1e}\xi\alpha_{1e}\mathrm{e}^{-\mathrm{i}\alpha_{1e}H}, T_{0610} = 2\mu_{1e}\xi\alpha_{1e}\mathrm{e}^{\mathrm{i}\alpha_{1e}H},\\
&T_{0611} = \mu_{1e}(\xi^2 - \beta_{1e}^2)\mathrm{e}^{-\mathrm{i}\beta_{1e}H}, T_{0612} = \mu_{1e}(\xi^2 - \beta_{1e}^2)\mathrm{e}^{\mathrm{i}\beta_{1e}H}, T_{0701} = -\lambda_1 \mathrm{e}^{-\lambda_1 H}, T_{0701} = -\lambda_2 \mathrm{e}^{-\lambda_2 H}, T_{0703} = -\lambda_3 \mathrm{e}^{-\lambda_3 H}, T_{0704} = \lambda_1 \mathrm{e}^{\lambda_1 H},\\
&T_{0705} = \lambda_2 \mathrm{e}^{\lambda_2 H}, T_{0706} = \lambda_3 \mathrm{e}^{\lambda_3 H}, T_{0707} = \mathrm{i}\xi \mathrm{e}^{-rH}, T_{0708} = \mathrm{i}\xi \mathrm{e}^{rH}, T_{0709} = \mathrm{i}\alpha_{1e}\mathrm{e}^{-\mathrm{i}\alpha_{1e}H}, T_{0710} = -\mathrm{i}\alpha_{1e}\mathrm{e}^{\mathrm{i}\alpha_{1e}H},\\
&T_{0711} = -\mathrm{i}\xi\mathrm{e}^{-\mathrm{i}\beta_{1e}H}, T_{0712} = -\mathrm{i}\xi\mathrm{e}^{\mathrm{i}\beta_{1e}H}, T_{0801} = \mathrm{i}\xi\mathrm{e}^{-\lambda_1 H}, T_{0802} = \mathrm{i}\xi\mathrm{e}^{-\lambda_2 H}, T_{0803} = \mathrm{i}\xi\mathrm{e}^{-\lambda_3 H}, T_{0804} = \mathrm{i}\xi\mathrm{e}^{\lambda_1 H}, T_{0805} = \mathrm{i}\xi\mathrm{e}^{\lambda_2 H},\\
&T_{0806} = \mathrm{i}\xi\mathrm{e}^{\lambda_3 H}, T_{0807} = r\mathrm{e}^{-rH}, T_{0808} = -r\mathrm{e}^{rH}, T_{0809} = -\mathrm{i}\xi\mathrm{e}^{-\mathrm{i}\alpha_{1e}H}, T_{0810} = -\mathrm{i}\xi\mathrm{e}^{\mathrm{i}\alpha_{1e}H}, T_{0811} = -\mathrm{i}\beta_{1e}\mathrm{e}^{-\mathrm{i}\beta_{1e}H},\\
&T_{0812} = \mathrm{i}\beta_{1e}\mathrm{e}^{\mathrm{i}\beta_{1e}H}, T_{0901} = \lambda_1(1-\delta_{p1}^l)\mathrm{e}^{-\lambda_1 H}, T_{0902} = \lambda_2(1-\delta_{p2}^l)\mathrm{e}^{-\lambda_2 H}, T_{0903} = \lambda_3(1-\delta_{p3}^l)\mathrm{e}^{-\lambda_3 H},\\
&T_{0904} = \lambda_1(\delta_{p1}^l - 1)\mathrm{e}^{\lambda_1 H}, T_{0905} = \lambda_2(\delta_{p2}^l - 1)\mathrm{e}^{\lambda_2 H}, T_{0906} = \lambda_3(\delta_{p3}^l - 1)\mathrm{e}^{\lambda_3 H}, T_{0907} = \mathrm{i}\xi(\delta_s^l - 1)\mathrm{e}^{-rH},\\
&T_{0908} = \mathrm{i}\xi(\delta_s^l - 1)\mathrm{e}^{rH}, T_{1001} = \lambda_1(1-\delta_{p1}^g)\mathrm{e}^{-\lambda_1 H}, T_{1002} = \lambda_2(1-\delta_{p2}^g)\mathrm{e}^{-\lambda_2 H}, T_{1003} = \lambda_3(1-\delta_{p3}^g)\mathrm{e}^{-\lambda_3 H},\\
&T_{1004} = \lambda_1(\delta_{p1}^g - 1)\mathrm{e}^{\lambda_1 H}, T_{1005} = \lambda_2(\delta_{p2}^g - 1)\mathrm{e}^{\lambda_2 H}, T_{1006} = \lambda_3(\delta_{p3}^g - 1)\mathrm{e}^{\lambda_3 H}, T_{1007} = \mathrm{i}\xi(\delta_s^g - 1)\mathrm{e}^{-rH},\\
&T_{1008} = \mathrm{i}\xi(\delta_s^g - 1)\mathrm{e}^{rH}, T_{1101} = \mathrm{i}\xi\left(\delta_{p1}^l - 1\right)\mathrm{e}^{-\lambda_1 H}, T_{1102} = \mathrm{i}\xi\left(\delta_{p2}^l - 1\right)\mathrm{e}^{-\lambda_2 H}, T_{1103} = \mathrm{i}\xi\left(\delta_{p3}^l - 1\right)\mathrm{e}^{-\lambda_3 H},\\
&T_{1104} = \mathrm{i}\xi\left(\delta_{p1}^l - 1\right)\mathrm{e}^{\lambda_1 H}, T_{1105} = \mathrm{i}\xi\left(\delta_{p2}^l - 1\right)\mathrm{e}^{\lambda_2 H}, T_{1106} = \mathrm{i}\xi\left(\delta_{p3}^l - 1\right)\mathrm{e}^{\lambda_3 H}, T_{1107} = r\left(\delta_s^l - 1\right)\mathrm{e}^{-rH},\\
&T_{1108} = r\left(1 - \delta_s^l\right)\mathrm{e}^{rH}, T_{1201} = \mathrm{i}\xi\left(\delta_{p1}^g - 1\right)\mathrm{e}^{-\lambda_1 H}, T_{1202} = \mathrm{i}\xi\left(\delta_{p2}^g - 1\right)\mathrm{e}^{-\lambda_2 H}, T_{1203} = \mathrm{i}\xi\left(\delta_{p3}^g - 1\right)\mathrm{e}^{-\lambda_3 H},
\end{aligned}
$$

$$T_{1204}=\mathrm{i}\xi\left(\delta_{p1}^{g}-1\right)\mathrm{e}^{\lambda_1 H},\ T_{1205}=\mathrm{i}\xi\left(\delta_{p2}^{g}-1\right)\mathrm{e}^{\lambda_2 H},\ T_{1206}=\mathrm{i}\xi\left(\delta_{p3}^{g}-1\right)\mathrm{e}^{\lambda_3 H},\ T_{1207}=r\left(\delta_{s}^{g}-1\right)\mathrm{e}^{-rH},$$

$$T_{1208}=r\left(1-\delta_{s}^{g}\right)\mathrm{e}^{rH},\ T_{1309}=-\left[\lambda_{1e}\xi^2+\alpha_{1e}^2(\lambda_{1e}+2\mu_{1e})\right]\mathrm{e}^{-\mathrm{i}\alpha_{1e}\left(H+h_{w1}\right)},\ T_{1310}=-\left[\lambda_{1e}\xi^2+\alpha_{1e}^2(\lambda_{1e}+2\mu_{1e})\right]\mathrm{e}^{\mathrm{i}\alpha_{1e}\left(H+h_{w1}\right)},$$

$$T_{1311}=2\mu_{1e}\xi\beta_{1e}\mathrm{e}^{-\mathrm{i}\beta_{1e}\left(H+h_{w1}\right)},\ T_{1312}=-2\mu_{1e}\xi\beta_{1e}\mathrm{e}^{-\mathrm{i}\beta_{1e}\left(H+h_{w1}\right)},\ T_{1313}=\left[\lambda_{2e}\xi^2+\alpha_{2e}^2(\lambda_{2e}+2\mu_{2e})\right]\mathrm{e}^{-\mathrm{i}\alpha_{2e}\left(H+h_{w1}\right)},$$

$$T_{1314}=\left[\lambda_{2e}\xi^2+\alpha_{2e}^2(\lambda_{2e}+2\mu_{2e})\right]\mathrm{e}^{\mathrm{i}\alpha_{2e}\left(H+h_{w1}\right)},\ T_{1315}=-2\mu_{2e}\xi\beta_{2e}\mathrm{e}^{-\mathrm{i}\beta_{2e}\left(H+h_{w1}\right)},\ T_{1316}=2\mu_{2e}\xi\beta_{2e}\mathrm{e}^{\mathrm{i}\beta_{2e}\left(H+h_{w1}\right)},$$

$$T_{1409}=2\mu_{1e}\xi\alpha_{1e}\mathrm{e}^{-\mathrm{i}\alpha_{1e}\left(H+h_{w1}\right)},\ T_{1410}=-2\mu_{1e}\xi\alpha_{1e}\mathrm{e}^{\mathrm{i}\alpha_{1e}\left(H+h_{w1}\right)},\ T_{1411}=\mu_{1e}\left(\beta_{1e}^2-\xi^2\right)\mathrm{e}^{-\mathrm{i}\beta_{1e}\left(H+h_{w1}\right)},$$

$$T_{1412}=\mu_{1e}\left(\beta_{1e}^2-\xi^2\right)\mathrm{e}^{\mathrm{i}\beta_{1e}\left(H+h_{w1}\right)},\ T_{1413}=-2\mu_{2e}\xi\alpha_{2e}\mathrm{e}^{-\mathrm{i}\alpha_{2e}\left(H+h_{w1}\right)},\ T_{1414}=2\mu_{2e}\xi\alpha_{2e}\mathrm{e}^{\mathrm{i}\alpha_{2e}\left(H+h_{w1}\right)},$$

$$T_{1415}=\mu_{2e}\left(\xi^2-\beta_{2e}^2\right)\mathrm{e}^{-\mathrm{i}\beta_{2e}\left(H+h_{w1}\right)},\ T_{1416}=\mu_{2e}\left(\xi^2-\beta_{2e}^2\right)\mathrm{e}^{\mathrm{i}\beta_{2e}\left(H+h_{w1}\right)},\ T_{1509}=-\mathrm{i}\alpha_{1e}\mathrm{e}^{-\mathrm{i}\alpha_{1e}\left(H+h_{w1}\right)},$$

$$T_{1510}=\mathrm{i}\alpha_{1e}\mathrm{e}^{\mathrm{i}\alpha_{1e}\left(H+h_{w1}\right)},\ T_{1511}=\mathrm{i}\xi\mathrm{e}^{-\mathrm{i}\beta_{1e}\left(H+h_{w1}\right)},\ T_{1512}=\mathrm{i}\xi\mathrm{e}^{\mathrm{i}\beta_{1e}\left(H+h_{w1}\right)},\ T_{1513}=\mathrm{i}\alpha_{2e}\mathrm{e}^{-\mathrm{i}\alpha_{2e}\left(H+h_{w1}\right)},$$

$$T_{1514}=-\mathrm{i}\alpha_{2e}\mathrm{e}^{\mathrm{i}\alpha_{2e}\left(H+h_{w1}\right)},\ T_{1515}=-\mathrm{i}\xi\mathrm{e}^{-\mathrm{i}\beta_{2e}\left(H+h_{w1}\right)},\ T_{1516}=-\mathrm{i}\xi\mathrm{e}^{\mathrm{i}\beta_{2e}\left(H+h_{w1}\right)},\ T_{1609}=\mathrm{i}\xi\mathrm{e}^{-\mathrm{i}\alpha_{1e}\left(H+h_{w1}\right)},$$

$$T_{1610}=\mathrm{i}\xi\mathrm{e}^{\mathrm{i}\alpha_{1e}\left(H+h_{w1}\right)},\ T_{1611}=\mathrm{i}\beta_{1e}\mathrm{e}^{-\mathrm{i}\beta_{1e}\left(H+h_{w1}\right)},\ T_{1612}=-\mathrm{i}\beta_{1e}\mathrm{e}^{\mathrm{i}\beta_{1e}\left(H+h_{w1}\right)},\ T_{1613}=-\mathrm{i}\xi\mathrm{e}^{-\mathrm{i}\alpha_{2e}\left(H+h_{w1}\right)},$$

$$T_{1614}=-\mathrm{i}\xi\mathrm{e}^{\mathrm{i}\alpha_{2e}\left(H+h_{w1}\right)},\ T_{1615}=-\mathrm{i}\beta_{2e}\mathrm{e}^{-\mathrm{i}\beta_{2e}\left(H+h_{w1}\right)},\ T_{1616}=\mathrm{i}\beta_{2e}\mathrm{e}^{\mathrm{i}\beta_{2e}\left(H+h_{w1}\right)},$$

$$T_{1713}=-\left[\lambda_{2e}\xi^2+\alpha_{2e}^2(\lambda_{2e}+2\mu_{2e})\right]\mathrm{e}^{-\mathrm{i}\alpha_{2e}\left(H+h_{w1}+h_{w2}\right)},\ T_{1714}=-\left[\lambda_{2e}\xi^2+\alpha_{2e}^2(\lambda_{2e}+2\mu_{2e})\right]\mathrm{e}^{\mathrm{i}\alpha_{2e}\left(H+h_{w1}+h_{w2}\right)},$$

$$T_{1715}=2\mu_{2e}\xi\beta_{2e}\mathrm{e}^{-\mathrm{i}\beta_{2e}\left(H+h_{w1}+h_{w2}\right)},\ T_{1716}=-2\mu_{2e}\xi\beta_{2e}\mathrm{e}^{-\mathrm{i}\beta_{2e}\left(H+h_{w1}+h_{w2}\right)},\ T_{1717}=\left[\lambda_{3e}\xi^2+\alpha_{3e}^2(\lambda_{3e}+2\mu_{3e})\right]\mathrm{e}^{-\mathrm{i}\alpha_{3e}\left(H+h_{w1}+h_{w2}\right)},$$

$$T_{1718}=\left[\lambda_{3e}\xi^2+\alpha_{3e}^2(\lambda_{3e}+2\mu_{3e})\right]\mathrm{e}^{\mathrm{i}\alpha_{3e}\left(H+h_{w1}+h_{w2}\right)},\ T_{1719}=-2\mu_{3e}\xi\beta_{3e}\mathrm{e}^{-\mathrm{i}\beta_{3e}\left(H+h_{w1}+h_{w2}\right)},\ T_{1720}=2\mu_{3e}\xi\beta_{3e}\mathrm{e}^{\mathrm{i}\beta_{3e}\left(H+h_{w1}+h_{w2}\right)},$$

$$T_{1813}=2\mu_{2e}\xi\alpha_{2e}\mathrm{e}^{-\mathrm{i}\alpha_{2e}\left(H+h_{w1}+h_{w2}\right)},\ T_{1814}=-2\mu_{2e}\xi\alpha_{2e}\mathrm{e}^{\mathrm{i}\alpha_{2e}\left(H+h_{w1}+h_{w2}\right)},\ T_{1815}=\mu_{2e}\left(\beta_{2e}^2-\xi^2\right)\mathrm{e}^{-\mathrm{i}\beta_{2e}\left(H+h_{w1}+h_{w2}\right)},$$

$$T_{1816}=\mu_{2e}\left(\beta_{2e}^2-\xi^2\right)\mathrm{e}^{\mathrm{i}\beta_{2e}\left(H+h_{w1}+h_{w2}\right)},\ T_{1817}=-2\mu_{3e}\xi\alpha_{3e}\mathrm{e}^{-\mathrm{i}\alpha_{3e}\left(H+h_{w1}+h_{w2}\right)},\ T_{1818}=2\mu_{3e}\xi\alpha_{3e}\mathrm{e}^{\mathrm{i}\alpha_{3e}\left(H+h_{w1}+h_{w2}\right)},$$

$$T_{1819}=\mu_{3e}\left(\xi^2-\beta_{3e}^2\right)\mathrm{e}^{-\mathrm{i}\beta_{3e}\left(H+h_{w1}+h_{w2}\right)},\ T_{1820}=\mu_{3e}\left(\xi^2-\beta_{3e}^2\right)\mathrm{e}^{\mathrm{i}\beta_{3e}\left(H+h_{w1}+h_{w2}\right)},\ T_{1913}=-\mathrm{i}\alpha_{2e}\mathrm{e}^{-\mathrm{i}\alpha_{2e}\left(H+h_{w1}+h_{w2}\right)},$$

$$T_{1914}=\mathrm{i}\alpha_{2e}\mathrm{e}^{\mathrm{i}\alpha_{2e}\left(H+h_{w1}+h_{w2}\right)},\ T_{1915}=\mathrm{i}\xi\mathrm{e}^{-\mathrm{i}\beta_{2e}\left(H+h_{w1}+h_{w2}\right)},\ T_{1916}=\mathrm{i}\xi\mathrm{e}^{\mathrm{i}\beta_{2e}\left(H+h_{w1}+h_{w2}\right)},\ T_{1917}=\mathrm{i}\alpha_{3e}\mathrm{e}^{-\mathrm{i}\alpha_{3e}\left(H+h_{w1}+h_{w2}\right)},$$

$$T_{1918}=-\mathrm{i}\alpha_{3e}\mathrm{e}^{\mathrm{i}\alpha_{3e}\left(H+h_{w1}+h_{w2}\right)},\ T_{1919}=-\mathrm{i}\xi\mathrm{e}^{-\mathrm{i}\beta_{3e}\left(H+h_{w1}+h_{w2}\right)},\ T_{1920}=-\mathrm{i}\xi\mathrm{e}^{\mathrm{i}\beta_{3e}\left(H+h_{w1}+h_{w2}\right)},\ T_{2013}=\mathrm{i}\xi\mathrm{e}^{-\mathrm{i}\alpha_{2e}\left(H+h_{w1}+h_{w2}\right)},$$

$$T_{2014}=\mathrm{i}\xi\mathrm{e}^{\mathrm{i}\alpha_{2e}\left(H+h_{w1}+h_{w2}\right)},\ T_{2015}=\mathrm{i}\beta_{2e}\mathrm{e}^{-\mathrm{i}\beta_{2e}\left(H+h_{w1}+h_{w2}\right)},\ T_{2016}=-\mathrm{i}\beta_{2e}\mathrm{e}^{\mathrm{i}\beta_{2e}\left(H+h_{w1}+h_{w2}\right)},\ T_{2017}=-\mathrm{i}\xi\mathrm{e}^{-\mathrm{i}\alpha_{3e}\left(H+h_{w1}+h_{w2}\right)},$$

$$T_{2018}=-\mathrm{i}\xi\mathrm{e}^{\mathrm{i}\alpha_{3e}\left(H+h_{w1}+h_{w2}\right)},\ T_{2019}=-\mathrm{i}\beta_{3e}\mathrm{e}^{-\mathrm{i}\beta_{3e}\left(H+h_{w1}+h_{w2}\right)},\ T_{2020}=\mathrm{i}\beta_{3e}\mathrm{e}^{\mathrm{i}\beta_{3e}\left(H+h_{w1}+h_{w2}\right)},$$

$$T_{2117}=-\left[\lambda_{3e}\xi^2+\alpha_{3e}^2(\lambda_{3e}+2\mu_{3e})\right]\mathrm{e}^{-\mathrm{i}\alpha_{3e}\left(H+h_{w1}+h_{w2}+h_{w3}\right)},\ T_{2118}=-\left[\lambda_{3e}\xi^2+\alpha_{3e}^2(\lambda_{3e}+2\mu_{3e})\right]\mathrm{e}^{\mathrm{i}\alpha_{3e}\left(H+h_{w1}+h_{w2}+h_{w3}\right)},$$

$$T_{2119}=2\mu_{3e}\xi\beta_{3e}\mathrm{e}^{-\mathrm{i}\beta_{3e}\left(H+h_{w1}+h_{w2}+h_{w3}\right)},\ T_{2120}=-2\mu_{3e}\xi\beta_{3e}\mathrm{e}^{\mathrm{i}\beta_{3e}\left(H+h_{w1}+h_{w2}+h_{w3}\right)},\ T_{2121}=-\chi_1\mathrm{e}^{-\lambda_1\left(H+h_{w1}+h_{w2}+h_{w3}\right)},$$

$$T_{2122}=-\chi_2\mathrm{e}^{-\lambda_2\left(H+h_{w1}+h_{w2}+h_{w3}\right)},\ T_{2123}=-\chi_3\mathrm{e}^{-\lambda_3\left(H+h_{w1}+h_{w2}+h_{w3}\right)},\ T_{2124}=-\chi_1\mathrm{e}^{\lambda_1\left(H+h_{w1}+h_{w2}+h_{w3}\right)},$$

$$T_{2125}=-\chi_2\mathrm{e}^{\lambda_2\left(H+h_{w1}+h_{w2}+h_{w3}\right)},\ T_{2126}=-\chi_3\mathrm{e}^{\lambda_3\left(H+h_{w1}+h_{w2}+h_{w3}\right)},\ T_{2127}=2\mu_p\mathrm{i}\xi r\mathrm{e}^{-r\left(HH+h_{w1}+h_{w2}+h_{w3}\right)},$$

$$T_{2128}=-2\mu_p\mathrm{i}\xi r\mathrm{e}^{r\left(H+h_{w1}+h_{w2}+h_{w3}\right)},\ T_{2217}=2\mu_{3e}\xi\alpha_{3e}\mathrm{e}^{-\mathrm{i}\alpha_{3e}\left(H+h_{w1}+h_{w2}+h_{w3}\right)},\ T_{2218}=-2\mu_{3e}\xi\alpha_{3e}\mathrm{e}^{\mathrm{i}\alpha_{3e}\left(H+h_{w1}+h_{w2}+h_{w3}\right)},$$

$$T_{2219}=\mu_{3e}(\beta_{3e}^2-\xi^2)\mathrm{e}^{-\mathrm{i}\beta_{3e}\left(H+h_{w1}+h_{w2}+h_{w3}\right)},\ T_{2220}=\mu_{3e}(\beta_{3e}^2-\xi^2)\mathrm{e}^{\mathrm{i}\beta_{3e}\left(H+h_{w1}+h_{w2}+h_{w3}\right)},\ T_{2221}=2\mu_p\mathrm{i}\xi\lambda_1\mathrm{e}^{-\lambda_1\left(H+h_{w1}+h_{w2}+h_{w3}\right)},$$

$$T_{2222}=2\mu_p\mathrm{i}\xi\lambda_2\mathrm{e}^{-\lambda_2\left(H+h_{w1}+h_{w2}+h_{w3}\right)},\ T_{2223}=2\mu_p\mathrm{i}\xi\lambda_3\mathrm{e}^{-\lambda_3\left(H+h_{w1}+h_{w2}+h_{w3}\right)},\ T_{2224}=-2\mu_p\mathrm{i}\xi\lambda_1\mathrm{e}^{\lambda_1\left(H+h_{w1}+h_{w2}+h_{w3}\right)},$$

$$T_{2225}=-2\mu_p \mathrm{i}\xi\lambda_2 \mathrm{e}^{\lambda_2(H+h_{w1}+h_{w2}+h_{w3})},\ T_{2226}=-2\mu_p \mathrm{i}\xi\lambda_3 \mathrm{e}^{\lambda_3(H+h_{w1}+h_{w2}+h_{w3})},\ T_{2227}=\mu_p(r^2+\xi^2)\mathrm{e}^{-r(H+h_{w1}+h_{w2}+h_{w3})}$$

$$T_{2228}=\mu_p(r^2+\xi^2)\mathrm{e}^{r(H+h_{w1}+h_{w2}+h_{w3})},\ T_{2317}=-\mathrm{i}\alpha_{3e}\mathrm{e}^{-\mathrm{i}\alpha_{3e}(H+h_{w1}+h_{w2}+h_{w3})},\ T_{2318}=\mathrm{i}\alpha_{3e}\mathrm{e}^{\mathrm{i}\alpha_{3e}(H+h_{w1}+h_{w2}+h_{w3})},$$

$$T_{2319}=\mathrm{i}\xi\mathrm{e}^{-\mathrm{i}\beta_{3e}(H+h_{w1}+h_{w2}+h_{w3})},\ T_{2320}=\mathrm{i}\xi\mathrm{e}^{\mathrm{i}\beta_{3e}(H+h_{w1}+h_{w2}+h_{w3})},\ T_{2321}=\lambda_1\mathrm{e}^{-\lambda_1(H+h_{w1}+h_{w2}+h_{w3})},$$

$$T_{2322}=\lambda_2\mathrm{e}^{-\lambda_2(H+h_{w1}+h_{w2}+h_{w3})},\ T_{2323}=\lambda_3\mathrm{e}^{-\lambda_3(H+h_{w1}+h_{w2}+h_{w3})},\ T_{2324}=-\lambda_1\mathrm{e}^{\lambda_1(H+h_{w1}+h_{w2}+h_{w3})},$$

$$T_{2325}=-\lambda_2\mathrm{e}^{\lambda_2(H+h_{w1}+h_{w2}+h_{w3})},\ T_{2326}=-\lambda_3\mathrm{e}^{\lambda_3(H+h_{w1}+h_{w2}+h_{w3})},\ T_{2327}=-\mathrm{i}\xi\mathrm{e}^{-r(H+h_{w1}+h_{w2}+h_{w3})},$$

$$T_{2328}=-\mathrm{i}\xi\mathrm{e}^{r(H+h_{w1}+h_{w2}+h_{w3})},\ T_{2417}=\mathrm{i}\xi\mathrm{e}^{-\mathrm{i}\alpha_{3e}(H+h_{w1}+h_{w2}+h_{w3})},\ T_{2418}=\mathrm{i}\xi\mathrm{e}^{\mathrm{i}\alpha_{3e}(H+h_{w1}+h_{w2}+h_{w3})},$$

$$T_{2419}=\mathrm{i}\beta_{3e}\mathrm{e}^{-\mathrm{i}\beta_{3e}(H+h_{w1}+h_{w2}+h_{w3})},\ T_{2420}=-\mathrm{i}\beta_{3e}\mathrm{e}^{\mathrm{i}\beta_{3e}(H+h_{w1}+h_{w2}+h_{w3})},\ T_{2421}=-\mathrm{i}\xi\mathrm{e}^{-\lambda_1(H+h_{w1}+h_{w2}+h_{w3})},$$

$$T_{2422}=-\mathrm{i}\xi\mathrm{e}^{-\lambda_2(H+h_{w1}+h_{w2}+h_{w3})},\ T_{2423}=-\mathrm{i}\xi\mathrm{e}^{-\lambda_3(H+h_{w1}+h_{w2}+h_{w3})},\ T_{2424}=-\mathrm{i}\xi\mathrm{e}^{\lambda_1(H+h_{w1}+h_{w2}+h_{w3})},$$

$$T_{2425}=-\mathrm{i}\xi\mathrm{e}^{\lambda_2(H+h_{w1}+h_{w2}+h_{w3})},\ T_{2426}=-\mathrm{i}\xi\mathrm{e}^{\lambda_3(H+h_{w1}+h_{w2}+h_{w3})},\ T_{2427}=-r\mathrm{e}^{-r(H+h_{w1}+h_{w2}+h_{w3})},\ T_{2428}=r\mathrm{e}^{r(H+h_{w1}+h_{w2}+h_{w3})},$$

$$T_{2521}=\lambda_1(\delta_{p1}^{l}-1)\mathrm{e}^{-\lambda_1(H+h_{w1}+h_{w2}+h_{w3})},\ T_{2522}=\lambda_2(\delta_{p2}^{l}-1)\mathrm{e}^{-\lambda_2(H+h_{w1}+h_{w2}+h_{w3})},\ T_{2523}=\lambda_3(\delta_{p3}^{l}-1)\mathrm{e}^{-\lambda_3(H+h_{w1}+h_{w2}+h_{w3})},$$

$$T_{2524}=\lambda_1(1-\delta_{p1}^{l})\mathrm{e}^{\lambda_1(H+h_{w1}+h_{w2}+h_{w3})},\ T_{2525}=\lambda_2(1-\delta_{p2}^{l})\mathrm{e}^{\lambda_2(H+h_{w1}+h_{w2}+h_{w3})},\ T_{2526}=\lambda_3(1-\delta_{p3}^{l})\mathrm{e}^{\lambda_3(H+h_{w1}+h_{w2}+h_{w3})},$$

$$T_{2527}=\mathrm{i}\xi(1-\delta_{s}^{l})\mathrm{e}^{-r(H+h_{w1}+h_{w2}+h_{w3})},\ T_{2528}=\mathrm{i}\xi(1-\delta_{s}^{l})\mathrm{e}^{r(H+h_{w1}+h_{w2}+h_{w3})},\ T_{2621}=\lambda_1(\delta_{p1}^{g}-1)\mathrm{e}^{-\lambda_1(H+h_{w1}+h_{w2}+h_{w3})},$$

$$T_{2622}=\lambda_2(\delta_{p2}^{g}-1)\mathrm{e}^{-\lambda_2(H+h_{w1}+h_{w2}+h_{w3})},\ T_{2623}=\lambda_3(\delta_{p3}^{g}-1)\mathrm{e}^{-\lambda_3(H+h_{w1}+h_{w2}+h_{w3})},\ T_{2624}=\lambda_1(1-\delta_{p1}^{g})\mathrm{e}^{\lambda_1(H+h_{w1}+h_{w2}+h_{w3})},$$

$$T_{2625}=\lambda_2(1-\delta_{p2}^{g})\mathrm{e}^{\lambda_2(H+h_{w1}+h_{w2}+h_{w3})},\ T_{2626}=\lambda_3(1-\delta_{p3}^{g})\mathrm{e}^{\lambda_3(H+h_{w1}+h_{w2}+h_{w3})},\ T_{2627}=\mathrm{i}\xi(1-\delta_{s}^{g})\mathrm{e}^{-r(H+h_{w1}+h_{w2}+h_{w3})},$$

$$T_{2628}=\mathrm{i}\xi(1-\delta_{s}^{g})\mathrm{e}^{r(H+h_{w1}+h_{w2}+h_{w3})},$$

$$T_{2721}=\mathrm{i}\xi\left(\delta_{p1}^{l}-1\right)\mathrm{e}^{-\lambda_1\left(H+h_{w1}+h_{w2}+h_{w3}\right)},\ T_{2722}=\mathrm{i}\xi\left(\delta_{p2}^{l}-1\right)\mathrm{e}^{-\lambda_2\left(H+h_{w1}+h_{w2}+h_{w3}\right)},$$

$$T_{2723}=\mathrm{i}\xi\left(\delta_{p3}^{l}-1\right)\mathrm{e}^{-\lambda_3\left(H+h_{w1}+h_{w2}+h_{w3}\right)},\ T_{2724}=\mathrm{i}\xi\left(\delta_{p1}^{l}-1\right)\mathrm{e}^{\lambda_1\left(H+h_{w1}+h_{w2}+h_{w3}\right)},\ T_{2725}=\mathrm{i}\xi\left(\delta_{p2}^{l}-1\right)\mathrm{e}^{\lambda_2\left(H+h_{w1}+h_{w2}+h_{w3}\right)},$$

$$T_{2726}=\mathrm{i}\xi\left(\delta_{p3}^{l}-1\right)\mathrm{e}^{\lambda_3\left(H+h_{w1}+h_{w2}+h_{w3}\right)},\ T_{2727}=r\left(\delta_{s}^{l}-1\right)\mathrm{e}^{-r\left(H+h_{w1}+h_{w2}+h_{w3}\right)},\ T_{2728}=r\left(1-\delta_{s}^{l}\right)\mathrm{e}^{r\left(H+h_{w1}+h_{w2}+h_{w3}\right)},$$

$$T_{2821}=\mathrm{i}\xi\left(\delta_{p1}^{g}-1\right)\mathrm{e}^{-\lambda_1\left(H+h_{w1}+h_{w2}+h_{w3}\right)},\ T_{2822}=\mathrm{i}\xi\left(\delta_{p2}^{g}-1\right)\mathrm{e}^{-\lambda_2\left(H+h_{w1}+h_{w2}+h_{w3}\right)},$$

$$T_{2823}=\mathrm{i}\xi\left(\delta_{p3}^{g}-1\right)\mathrm{e}^{-\lambda_3\left(H+h_{w1}+h_{w2}+h_{w3}\right)},\ T_{2824}=\mathrm{i}\xi\left(\delta_{p1}^{g}-1\right)\mathrm{e}^{\lambda_1\left(H+h_{w1}+h_{w2}+h_{w3}\right)},\ T_{2825}=\mathrm{i}\xi\left(\delta_{p2}^{g}-1\right)\mathrm{e}^{\lambda_2\left(H+h_{w1}+h_{w2}+h_{w3}\right)},$$

$$T_{2826}=\mathrm{i}\xi\left(\delta_{p3}^{g}-1\right)\mathrm{e}^{\lambda_3\left(H+h_{w1}+h_{w2}+h_{w3}\right)},\ T_{2827}=r\left(\delta_{s}^{g}-1\right)\mathrm{e}^{-r\left(H+h_{w1}+h_{w2}+h_{w3}\right)},\ T_{2828}=r\left(1-\delta_{s}^{g}\right)\mathrm{e}^{r\left(H+h_{w1}+h_{w2}+h_{w3}\right)},$$

$$T_{2921}=\chi_1\mathrm{e}^{-\lambda_1\left(H+h_{w1}+h_{w2}+h_{w3}+h\right)},\ T_{2922}=\chi_2\mathrm{e}^{-\lambda_2\left(H+h_{w1}+h_{w2}+h_{w3}+h\right)},\ T_{2923}=\chi_3\mathrm{e}^{-\lambda_3\left(H+h_{w1}+h_{w2}+h_{w3}+h\right)},$$

$$T_{2924}=\chi_1\mathrm{e}^{\lambda_1\left(H+h_{w1}+h_{w2}+h_{w3}+h\right)},\ T_{2925}=\chi_2\mathrm{e}^{\lambda_2\left(H+h_{w1}+h_{w2}+h_{w3}+h\right)},\ T_{2926}=\chi_3\mathrm{e}^{\lambda_3\left(H+h_{w1}+h_{w2}+h_{w3}+h\right)},$$

$$T_{2927}=-2\mu_p \mathrm{i}\xi r\mathrm{e}^{-r\left(H+h_{w1}+h_{w2}+h_{w3}+h\right)},\ T_{2928}=2\mu_p \mathrm{i}\xi r\mathrm{e}^{r\left(H+h_{w1}+h_{w2}+h_{w3}+h\right)},\ T_{2929}=-\chi_1\mathrm{e}^{-\lambda_1\left(H+h_{w1}+h_{w2}+h_{w3}+h\right)},$$

$$T_{2930}=-\chi_2\mathrm{e}^{-\lambda_2\left(H+h_{w1}+h_{w2}+h_{w3}+h\right)},\ T_{2931}=-\chi_3\mathrm{e}^{-\lambda_3\left(H+h_{w1}+h_{w2}+h_{w3}+h\right)},\ T_{2932}=2\mu_p \mathrm{i}\xi r\mathrm{e}^{-r\left(H+h_{w1}+h_{w2}+h_{w3}+h\right)},$$

$$T_{3021}=-2\mu_p \mathrm{i}\xi\lambda_1\mathrm{e}^{-\lambda_1\left(H+h_{w1}+h_{w2}+h_{w3}+h\right)},\ T_{3022}=-2\mu_p \mathrm{i}\xi\lambda_2\mathrm{e}^{-\lambda_2\left(H+h_{w1}+h_{w2}+h_{w3}+h\right)},\ T_{3023}=-2\mu_p \mathrm{i}\xi\lambda_3\mathrm{e}^{-\lambda_3\left(H+h_{w1}+h_{w2}+h_{w3}+h\right)},$$

$$T_{3024}=2\mu_p \mathrm{i}\xi\lambda_1\mathrm{e}^{\lambda_1\left(H+h_{w1}+h_{w2}+h_{w3}+h\right)},\ T_{3025}=2\mu_p \mathrm{i}\xi\lambda_2\mathrm{e}^{\lambda_2\left(H+h_{w1}+h_{w2}+h_{w3}+h\right)},\ T_{3026}=2\mu_p \mathrm{i}\xi\lambda_3\mathrm{e}^{\lambda_3\left(H+h_{w1}+h_{w2}+h_{w3}+h\right)},$$

$T_{3027} = -\mu_p(r^2+\xi^2)\mathrm{e}^{-r\left(H+h_{w1}+h_{w2}+h_{w3}+h\right)}$, $T_{3028} = -\mu_p(r^2+\xi^2)\mathrm{e}^{r\left(H+h_{w1}+h_{w2}+h_{w3}+h\right)}$,
$T_{3029} = 2\mu_p \mathrm{i}\xi\lambda_1\mathrm{e}^{-\lambda_1\left(H+h_{w1}+h_{w2}+h_{w3}+h\right)}$, $T_{3030} = 2\mu_p \mathrm{i}\xi\lambda_2\mathrm{e}^{-\lambda_2\left(H+h_{w1}+h_{w2}+h_{w3}+h\right)}$, $T_{3031} = 2\mu_p \mathrm{i}\xi\lambda_3\mathrm{e}^{-\lambda_3\left(H+h_{w1}+h_{w2}+h_{w3}+h\right)}$,
$T_{3032} = \mu_p(r^2+\xi^2)\mathrm{e}^{-r\left(H+h_{w1}+h_{w2}+h_{w3}+h\right)}$, $T_{3121} = -\lambda_1\mathrm{e}^{-\lambda_1\left(H+h_{w1}+h_{w2}+h_{w3}+h\right)}$, $T_{3122} = -\lambda_2\mathrm{e}^{-\lambda_2\left(H+h_{w1}+h_{w2}+h_{w3}+h\right)}$,
$T_{3123} = -\lambda_3\mathrm{e}^{-\lambda_3\left(H+h_{w1}+h_{w2}+h_{w3}+h\right)}$, $T_{3124} = \lambda_1\mathrm{e}^{\lambda_1\left(H+h_{w1}+h_{w2}+h_{w3}+h\right)}$, $T_{3125} = \lambda_2\mathrm{e}^{\lambda_2\left(H+h_{w1}+h_{w2}+h_{w3}+h\right)}$,
$T_{3126} = \lambda_3\mathrm{e}^{\lambda_3\left(H+h_{w1}+h_{w2}+h_{w3}+h\right)}$, $T_{3127} = \mathrm{i}\xi\mathrm{e}^{-r\left(H+h_{w1}+h_{w2}+h_{w3}+h\right)}$, $T_{3128} = \mathrm{i}\xi\mathrm{e}^{r\left(H+h_{w1}+h_{w2}+h_{w3}+h\right)}$,
$T_{3129} = \lambda_1\mathrm{e}^{-\lambda_1\left(H+h_{w1}+h_{w2}+h_{w3}+h\right)}$, $T_{3130} = \lambda_2\mathrm{e}^{-\lambda_2\left(H+h_{w1}+h_{w2}+h_{w3}+h\right)}$, $T_{3131} = \lambda_3\mathrm{e}^{-\lambda_3\left(H+h_{w1}+h_{w2}+h_{w3}+h\right)}$,
$T_{3132} = -\mathrm{i}\xi\mathrm{e}^{-r\left(H+h_{w1}+h_{w2}+h_{w3}+h\right)}$, $T_{3221} = \mathrm{i}\xi\mathrm{e}^{-\lambda_1\left(H+h_{w1}+h_{w2}+h_{w3}+h\right)}$, $T_{3222} = \mathrm{i}\xi\mathrm{e}^{-\lambda_2\left(H+h_{w1}+h_{w2}+h_{w3}+h\right)}$,
$T_{3223} = \mathrm{i}\xi\mathrm{e}^{-\lambda_3\left(H+h_{w1}+h_{w2}+h_{w3}+h\right)}$, $T_{3224} = \mathrm{i}\xi\mathrm{e}^{\lambda_1\left(H+h_{w1}+h_{w2}+h_{w3}+h\right)}$, $T_{3225} = \mathrm{i}\xi\mathrm{e}^{\lambda_2\left(H+h_{w1}+h_{w2}+h_{w3}+h\right)}$,
$T_{3226} = \mathrm{i}\xi\mathrm{e}^{\lambda_3\left(H+h_{w1}+h_{w2}+h_{w3}+h\right)}$, $T_{3227} = r\mathrm{e}^{-r\left(H+h_{w1}+h_{w2}+h_{w3}+h\right)}$, $T_{3228} = -r\mathrm{e}^{r\left(H+h_{w1}+h_{w2}+h_{w3}+h\right)}$,
$T_{3229} = -\mathrm{i}\xi\mathrm{e}^{-\lambda_1\left(H+h_{w1}+h_{w2}+h_{w3}+h\right)}$, $T_{3230} = -\mathrm{i}\xi\mathrm{e}^{-\lambda_2\left(H+h_{w1}+h_{w2}+h_{w3}+h\right)}$, $T_{3231} = -\mathrm{i}\xi\mathrm{e}^{-\lambda_3\left(H+h_{w1}+h_{w2}+h_{w3}+h\right)}$,
$T_{3232} = -r\mathrm{e}^{-r\left(H+h_{w1}+h_{w2}+h_{w3}+h\right)}$.